AD-A047 319 NAVAL POSTGRADUATE SCHOOL MONTEREY CALIF F/G 8/12
THE OPERATIONAL DETERMINATION OF WIND STRESS ON THE ARCTIC ICE --ETC(U)
SEP 77 L D ASHIM

UNCLASSIFIED NL

OF
AD
A047319



END
DATE FILMED
1-78
DDC

AD A047319

NAVAL POSTGRADUATE SCHOOL
Monterey, California



DDC
DEC 7 1977
F

THESIS

The Operational Determination of Wind Stress On the Arctic Ice Pack

by

Larry Dennis Ashim

September 1977

Thesis Advisor: W.W. Denner

Approved for public release; distribution unlimited

AD No.
DDC FILE COPY

SECURITY CLASSIFICATION OF THIS PAGE (When Data Entered)

REPORT DOCUMENTATION PAGE

READ INSTRUCTIONS BEFORE COMPLETING FORM

1. REPORT NUMBER

2. GOVT ACCESSION NO.

3. RECIPIENT'S CATALOG NUMBER

4. TITLE (and Subtitle)

The Operational Determination of Wind Stress on the Arctic Ice Pack.

5. TYPE OF REPORT & PERIOD COVERED

Master's Thesis, September 1977

6. PERFORMING ORG. REPORT NUMBER

7. AUTHOR(s)

Larry Dennis Ashim

8. CONTRACT OR GRANT NUMBER(s)

9. PERFORMING ORGANIZATION NAME AND ADDRESS

Naval Postgraduate School
Monterey, CA 93940

10. PROGRAM ELEMENT, PROJECT, TASK AREA & WORK UNIT NUMBERS

11. CONTROLLING OFFICE NAME AND ADDRESS

Naval Postgraduate School
Monterey, CA 93940

12. REPORT DATE

September 1977

13. NUMBER OF PAGES

79

14. MONITORING AGENCY NAME & ADDRESS(if different from Controlling Office)

Naval Postgraduate School
Monterey, CA 93940

78p.

15. SECURITY CLASS. (of this report)

Unclassified

15a. DECLASSIFICATION/DOWNGRADING SCHEDULE

16. DISTRIBUTION STATEMENT (of this Report)

Approved for public release; distribution unlimited

17. DISTRIBUTION STATEMENT (of the abstract entered in Block 20, if different from Report)

18. SUPPLEMENTARY NOTES

19. KEY WORDS (Continue on reverse side if necessary and identify by block number)

AIDJEX	Meteorological Analysis
Ice	Arctic Ice Pack
Models	Ice Dynamics
Air Sea Interaction	Ice Forecasting

20. ABSTRACT (Continue on reverse side if necessary and identify by block number)

The performance of routine FNWC sea level pressure analyses and forecasts in the Beaufort Sea is evaluated for driving an ice model. The geostrophic winds determined from the FNWC pressure fields are compared to geostrophic winds determined from the AIDJEX experiment observations. A simulation with the AIDJEX model has been run using FNWC sea level pressure analysis fields

DD FORM 1 JAN 73 1473 EDITION OF 1 NOV 65 IS OBSOLETE
S/N 0102-014-6601

SECURITY CLASSIFICATION OF THIS PAGE (When Data Entered)

251 450

LB

for the period 15 to 25 May 1975 and compared to the AIDJEX results. RMS sea level pressure errors of about 3 mb were found with analysis errors reduced by about 1 mb when one AIDJEX observation was included in the analysis. Geostrophic winds had speed differences of about 40% and direction differences of about 50°. The FNWC simulation with the AIDJEX model produced a position error of about 7 km for one station over the ten day run. Recommendations are made to improve the FNWC hemispheric fields in the Arctic for application to ice forecasting.

ACCESSION for
NTIS White Section
DDC Buff Section
UNANNOUNCED
JUSTIFICATION
BY
DISTRIBUTION/AVAILABILITY CODES
Dist. SPECIAL
A

Approved for public release; distribution unlimited

The Operational Determination of Wind Stress On the Arctic Ice Pack

by

Larry Dennis Ashim
Lieutenant, United States Navy
B.S., University of Kansas, 1972

Submitted in partial fulfillment of the
requirements for the degree of

MASTER OF SCIENCE IN OCEANOGRAPHY

from the

NAVAL POSTGRADUATE SCHOOL
September 1977

Author Larry D Ashim

Approved by: Warren A Denner
Thesis Advisor

Dale F Leslie (Rd)
Chairman, Department of Oceanography

Robert Fossum
Dean of Science and Engineering

ABSTRACT

The performance of routine FNWC sea level pressure analyses and forecasts in the Beaufort Sea is evaluated for driving an ice model. The geostrophic winds determined from the FNWC pressure fields are compared to geostrophic winds determined from the AIDJEX experiment observations. A simulation with the AIDJEX model has been run using FNWC sea level pressure analysis fields for the period 15 to 25 May 1975 and compared to the AIDJEX results.

RMS sea level pressure errors of about 3 mb were found with analysis errors reduced by about 1 mb when one AIDJEX observation was included in the analysis. Geostrophic winds had speed differences of about 40% and direction differences of about 50°. The FNWC simulation with the AIDJEX model produced a position error of about 7 km for one station over the ten day run.

Recommendations are made to improve the FNWC hemispheric fields in the Arctic for application to ice forecasting.

TABLE OF CONTENTS

I.	INTRODUCTION	9
	A. NATURE OF THE PROBLEM	10
	B. DESCRIPTION OF THE ARCTIC ICE PACK	13
II.	HISTORICAL BACKGROUND	16
III.	DESCRIPTION OF THE AIDJEX MODEL	19
IV.	EVALUATION OF FNWC SEA-LEVEL PRESSURE FIELD AND GEOSTROPHIC WINDS	24
	A. DESCRIPTION OF THE FIELDS BY INFORMATION BLENDING (FIB) TECHNIQUE	24
	B. SEA-LEVEL PRESSURE EVALUATION METHOD	26
	C. METHOD OF EVALUATION OF GEOSTROPHIC WINDS	29
	D. SIMULATION RESULTS	31
V.	CONCLUSIONS	36
VI.	RECOMMENDATIONS	39
APPENDIX A:	FIGURES	40
BIBLIOGRAPHY		75
INITIAL DISTRIBUTION LIST		78

LIST OF FIGURES

1.	Extent of Sea Ice in the Northern Hemisphere	40
2.	A Representative Thickness Distribution	41
3.	The AIDJEX Computational Grid	42
4.	Simplified Flow Diagram of FIB Technique	43
5.	AIDJEX Sea-Level Pressure Analysis for 1200GMT 18 May 1975	44
6.	FNWC Sea-Level Pressure Analysis for 1200GMT 18 May 1975	45
7.	FNWC RMS Pressure Error	46
8.	Time Series of Sea-Level Pressure at AIDJEX Main Camp	47
9.	FNWC RMS Pressure Error and Mean Pressure Error	51
10.	RMS Speed and Direction Differences	52
11.	Computed Air Stress Time Series at AIDJEX Main Camp	53
12.	Computed Air Stress Time Series at Node 3,7	55
13.	AIDJEX Computed Air Stress Field at 1200GMT 18 May 1975	57
14.	FNWC Computed Air Stress Field at 1200GMT 18 May 1975	58
15.	Trajectories of AIDJEX Main Camp	59
16.	Position Time Series of AIDJEX Main Camp	60
17.	Trajectories of Node 3,7	62
18.	Position Time Series of Node 3,7	63
19.	AIDJEX Computed Velocity Field at 1200GMT 18 May 1975	65
20.	AIDJEX Computed Stress Divergence Field at 1200GMT 18 May 1975	66
21.	FNWC Computed Velocity Field at 1200GMT 18 May 1975	67

22. FNWC Computed Stress Divergence Field at 1200GMT 18 May 1975 68

23. Velocity Time Series of AIDJEX Main Camp 69

24. AIDJEX Computed Air Stress Field at 1200GMT 22 May 1975 71

25. AIDJEX Computed Velocity Field at 1200GMT 22 May 1975 72

26. FNWC Computed Air Stress Field at 1200GMT 22 May 1975 73

27. FNWC Computed Velocity Field at 1200GMT 22 May 1975 74

ACKNOWLEDGEMENTS

This research was funded by the Office of Naval Research through the Arctic Chair in Marine Sciences at the Naval Postgraduate School. Data and computer facilities were provided by Fleet Numerical Weather Central. AIDJEX data were supplied by the AIDJEX project office which also provided the AIDJEX model. The author wishes to thank Mr. Don Thomas of AIDJEX whose assistance in adapting the model to the FNWC system was invaluable, and who also added innovative concepts in computer programming which smoothed over other problem areas. Appreciation is expressed to Dr. Warren W. Denner for his guidance in all aspects of the research and to Dr. Robert J. Renard for his thoughtful suggestions in preparation of the manuscript. And, a very special thanks to the author's wife Karen without whose secretarial skills and encouragement this thesis would not be possible.

I. INTRODUCTION

Recent developments have demonstrated the strategic importance of the Arctic to the security of America. Soviet Delta-class submarines are on patrol out of their homeport of Murmansk armed with nuclear tipped missiles able to strike the heartland of America from anywhere within the Arctic Ocean. Soviet strategy is to seek open spots in the ice pack as launch points for their attacks [Anonymous, 1977]. The Northern Sea Route represents a major Soviet strategic interest [Synhorst, 1973]. As reported in the Monterey Peninsula Herald, (1977), the Soviets have demonstrated their ability to penetrate to the North Pole with an atomic ice breaker and announced their intention to open a great circle shipping route through the Arctic Ocean, events which make their interest all the more ominous. German submarines in World War II demonstrated a threat to the Northern Sea Route by their operations in the Kara Sea [Synhorst, 1973]. In the event of war any attempts by U. S. submarines to counter the Soviet SSBN threat in the Arctic or sever the Soviet lines of communications via the Northern Sea Route must be aided by reliable knowledge of ice conditions in order to make acoustic performance predictions and optimum under-ice track routing.

The North Slope of Alaska holds a critical supply of America's lifeblood, oil. The Navy provides forecasts of ice conditions vital to the continued free passage of U. S.

maritime resupply vessels to this valuable area. Again, reliable ice forecasts are crucial to America's interests.

A. NATURE OF THE PROBLEM

A knowledge of ridge and lead formation and distribution are of importance in meeting several Navy requirements. For example, the long, smooth refrozen leads are the basic landing strips on the pack. Knowing the location and ice thickness of these refrozen leads would be of great help in carrying out scientific research and logistic support on the pack. In shallow areas such as the Chukchi Sea the ice keels beneath ridges can form a considerable hazard to under-ice navigation. Ice free leads or thin ice can act as places for emergency surfacing of a submarine. Penetration of the ice is impeded when the pack is under high internal stress. Combined with a knowledge of ice thickness, a knowledge of the stress state of the ice would aid in these decisions, and weapons and sensor deployment through the pack. A submariner might find accurate forecasts of these conditions very reassuring on a submerged transit of the Arctic.

The two features in the polar environment that most strongly influence underwater sound are the permanent ice cover and the sound speed structure of the water. The essentially positive sound speed gradient causes sound rays to be generally refracted upward and then reflected and/or scattered from the rough ice-water interface [Diachok, 1976]. Both high and low frequencies are rapidly attenuated, the former by scattering losses from the ice cover, the latter by the

fact that very low frequencies are not effectively trapped in the channel [Urick, 1975]. Recently it has been demonstrated that back-scattering strength is controlled virtually exclusively by the size and number of sea-ice ridges [Diachok, 1976].

The principal source of ambient noise in the Arctic and sub-Arctic water is large scale deformation of ice floes [Diachok, 1976]. When the ice is not continuous, as near the ice edge, noise levels 5 to 10 dB higher than those measured at the same sea state in ice-free water have been observed [Urick, 1975]. The mechanisms responsible are related to wind-generated ocean wave interactions with sea ice at the boundary [Diachok, 1976]. Under a continuous ice sheet with calm winds and rising temperatures very low levels of ambient noise, well below the lowest Knudsen curve for sea-state zero, have been found. On the other hand, levels some 40 dB higher have been observed when the ice had been cracking under falling air temperature [Urick, 1975]. The acoustic propagation and ambient noise factors are both important in under-ice navigation, submarine tracking and localization, and weapons performance.

In addition to its effect on the under-ice environment the ice cover has a significant effect on the climate of the Arctic by acting as a lid on the ocean. A typical mesoscale region in the ice pack can be expected to contain open water, young ice tens of centimeters in thickness, perennial and deformed ice a few meters thick. Of concern in atmospheric modeling is the fact that open water and thin ice can exert

a large influence on regional heat exchange rates. For example, results by Maykut [1976] indicate ice 0-40 cm thic allows a net heat exchange to the atmosphere one to two ord of magnitude greater than perennial ice a few meters thick. Ice thickness greater than 100 cm exhibit little change in heat flux as the ice thickens. In the Central Arctic durin winter, estimates of open water and young thin ice are less than 1% and 8 to 12%, respectively. Thus, even at this sma percentage the effects of these two ice conditions can begi to dominate the large scale heat exchange and alter boundar conditions. Atmospheric models which assume the ice cover is a continuous three meter layer may seriously underestima the heat input to the boundary layer.

At the present time the Navy ice prediction models are only intended to serve as an aid to hand analysis. The win drift model used by the Navy ice forecasting group at the Fleet Weather Facility, Suitland, Maryland, gives ice speed as a linear function of surface wind speed [Skiles, 1968]. Moving to the right of the wind, the drift angle is given a an inverse exponential function of wind speed. Under development is a model to provide daily wind drift after Shuleikin [1953] and growth after Zubov [1945] at 62 coast weather reporting stations [Gerson and Simpson, 1976, and Gerson, 1975]. Barnett [1976] has presented a scheme for estimating the general ice conditions during the shipping season of the North Slope sea route using the height of th 1000 mb surface at two geographic locations (52N, 100E, an 70N, 140E).

a large influence on regional heat exchange rates. For example, results by Maykut [1976] indicate ice 0-40 cm thick allows a net heat exchange to the atmosphere one to two orders of magnitude greater than perennial ice a few meters thick. Ice thickness greater than 100 cm exhibit little change in heat flux as the ice thickens. In the Central Arctic during winter, estimates of open water and young thin ice are less than 1% and 8 to 12%, respectively. Thus, even at this small percentage the effects of these two ice conditions can begin to dominate the large scale heat exchange and alter boundary conditions. Atmospheric models which assume the ice cover is a continuous three meter layer may seriously underestimate the heat input to the boundary layer.

At the present time the Navy ice prediction models are only intended to serve as an aid to hand analysis. The wind drift model used by the Navy ice forecasting group at the Fleet Weather Facility, Suitland, Maryland, gives ice speed as a linear function of surface wind speed [Skiles, 1968]. Moving to the right of the wind, the drift angle is given as an inverse exponential function of wind speed. Under development is a model to provide daily wind drift after Shuleikin [1953] and growth after Zubov [1945] at 62 coastal weather reporting stations [Gerson and Simpson, 1976, and Gerson, 1975]. Barnett [1976] has presented a scheme for estimating the general ice conditions during the shipping season of the North Slope sea route using the height of the 1000 mb surface at two geographic locations (52N, 100E, and 70N, 140E).

All these models are conceptually extremely simple in the light of our present understanding of the complexity of sea-ice dynamics and they will probably not be capable of meeting the expanding needs of the Navy for arctic ice forecasting. Several more complete dynamical models of the arctic ice pack have been formulated [Campbell, 1965; Coon, et al, 1977; Hibler, 1977]. Therefore, a new model is in order, but first an assessment of present Navy analysis and forecast fields in the Arctic is needed to determine if these are capable of meeting the needs of the more complex models.

B. DESCRIPTION OF THE ARCTIC ICE PACK

The Arctic ice pack forms a lid over most of the North Polar Sea, constantly changing its extent of coverage, patterns of motion and thickness distribution. The seasonal range of ice coverage is illustrated in Figure 1. Of note is the extreme variability of the position of the ice edge, resulting in a 20% change in the areal coverage, receding in summer far enough to allow a shipping season along the north coast of Siberia and the North Slope of Alaska.

The summer season brings melting to the central pack, reducing the average thickness by about one meter and producing large open water areas [Orvig, 1970]. These open water areas effectively reduce the large scale strength of the ice pack to zero and allow the floes to move freely.

While the day-to-day movement of individual ice floes resembles a random walk, the long term general circulation of the ice pack has a regular pattern. Two dominant features

are a trans-polar drift from the East Siberian Sea, across the North Pole, and out of the Arctic into the East Greenland Current, and an anti-cyclonic gyre in the Beaufort Sea. These large scale climatic motions resemble the atmospheric climatic circulation patterns in the same way that the lower latitude ocean circulations resemble climatic wind patterns [Campbell, 1965].

In contrast to the relatively free movement of the ice in the central pack, the coastal ice remains attached to land in winter, preventing longshore movement. The transition from zero velocity of the land fast ice to a velocity of a few centimeters/sec in the central pack occurs in the shear zone, normally found a few kilometers offshore where sharpe ice velocity gradients occur.

The central pack has an average thickness of about three meters and it is made up of individual floes with dimensions of a few meters to several hundred meters [Orvig, 1970]. In winter these floes are separated by ridges up to several meters high and interlaced with leads of open water up to 0.5 km wide and several kilometers long, leads which quickly refreeze to form large smooth areas of young ice which eventually form ridges and new floes. These ridges and leads are formed by the relative motion of the ice whose principal driving force is the wind. The nature of ridging is extremely complex. Reduced to a simple description, sea-ice ridges are rubble piles formed by collisions and shear interactions between adjacent floes. The ridges above level ice are accompanied by keels below the surface, keels which may

extend many times as deep as the ridge is high. Since on a large scale the ice is densely fractured it has little tensile strength and readily opens when subjected to a stretching or divergent strain [Pritchard and Colony, 1976].

II. HISTORICAL BACKGROUND

The modeling of ice dynamics can be divided into three categories; empirical modeling, small-scale analytical modeling and synoptic-scale analytic modeling. The empirical modeling began with the observations by Nansen during the drift of the Fram across the Arctic Ocean (1893-96), who observed that ice drift speed was about 2% of the wind speed and generally to the right of the wind direction at an average angle of 28°. Sverdrup, drifting with the ice pack in the Maud, (1919-25), found a wind factor for ice of 0.014 to 0.024 and a drift angle from 18° to 40°, the latter when the ice was loose in summer.

Zubov [1945] further developed the empirical relationship of wind and ice drift. His analysis of the drift of the Sedov yielded a wind factor of 0.015 and drift angle of 29°, which compare favorably with Nansen. Zubov further postulated that ice drift follows the sea-level isobars, i.e., it is parallel to the sea level geostrophic wind because the counter-clockwise turning of the wind through the atmospheric friction layer is approximately equivalent to the ice drift angle to the right of the surface wind.

Early work in analytic modeling of small-scale ice dynamics was done by Shuleikin [1953] who derived the force balance and motion of the ice due to the wind stress. However, his theories were limited to 10/10 ice coverage. Fukutomi [1948] treated ice drift by considering the effects of ice

concentration, roughness and ocean currents in an analytical model.

Modern high speed computers have made it practical to develop synoptic-scale ice drift models which span a broad range in complexity. Simplest are the wind drift models using empirical relationships. An example of the use of wind drift relationships is the numerical model developed by Knodle [1964], which combines Shuleikin's and Fukutomi's theories, yielding a wind drift field which is a function of ice concentration for Baffin Bay. The most complex are analytical models which consider the interactions within the pack ice. Because of the internal stresses transmitted through the ice pack a solution which neglects the interaction of the ice cannot completely describe the dynamics.

The first models which attempted to include the interaction of the ice assumed it to have a viscous nature. In formulating his ice circulation model Campbell [1965] considers individual ice floes as "... fluid elements with an average area which is small compared with the ocean area, [thus] the ice sheet may be viewed as a film of highly viscous fluid suspended between two less viscous fluids, air and water." While Campbell and several other authors have produced viscous models which describe the general circulation of ice in the Arctic, all have limitations, the most notable is their inability to model the coastal shear zone.

Hibler [1977] has developed a viscous model which simulates large scale (100 km) sea-ice dynamics; the model has been run for simulations 8 years in length. Since this model

is not hampered by numerical stability problems it is able to utilize large time steps (1 day) and thus perform long-term simulations, while still retaining the ability to be run in smaller time and space scales. This model incorporates an ice thickness evaluation which combines mean thickness and compactness. Despite his model's success Hibler states, "... particular elastic-plastic rheologies may well be more useful in reproducing many detailed small scale effects."

One of the most recent models, which takes a departure from viewing the ice as viscous in nature, is that formulated by the Arctic Ice Dynamics Joint Experiment (AIDJEX) program. It models the ice as an elastic-plastic material whose yield strength depends on the amount of thin ice present. A major difference between the plastic and fluid models is that the plastic material responds independently of the rate of the deformation [Coon, Hall and Pritchard, 1977]. In simulations covering periods of about 10 days the AIDJEX model has produced good results in describing both large and small scale features of ice dynamics and depicting the coastal shear zone [Coon, et al, 1977]. Because of the potential success of the AIDJEX model in addressing these important Navy requirements for ice forecasting, it was selected as a means of evaluating the Navy's atmospheric analysis and prognostic fields for use in an ice dynamics model.

III. DESCRIPTION OF THE AIDJEX MODEL

The AIDJEX ice model consists of three major parts: the momentum equation, a set of constitutive laws which describe the stress-strain behavior of the ice in the horizontal plane, and the ice thickness distribution [Coon, et al, 1976].

The first element of the model is the momentum equation which states that the acceleration of an element of ice of mass (m) is related to the air stress, ($\vec{\tau}_a$), the water stress ($\vec{\tau}_w$), the coriolis force, and the divergence of internal stresses ($\vec{\nabla} \cdot \bar{\bar{\sigma}}$). The momentum equation is written:

$$m\dot{\vec{v}} = \vec{\tau}_a + \vec{\tau}_w + \vec{\nabla} \cdot \bar{\bar{\sigma}} \quad -mf_c\hat{k}x\vec{v} + mf_c\hat{k}x\vec{v}_g \qquad (1)$$

where

$\vec{v}$ = ice velocity

$-mf_c\hat{k}x\vec{v}$ = coriolis force

f_c = coriolis parameter

$mf_c\hat{k}x\vec{v}_g$ = sea surface tilt force

$\vec{v}_g$ = geostrophic current

Air stress is computed as a quadratic function of the geostrophic wind [Pritchard, et al, 1976]:

$$\vec{\tau}_a = \rho_a C_D |\vec{U}| \underset{\sim}{B}_a \vec{U} \qquad (2)$$

where

ρ_a = air density

C_D = geostrophic drag coefficient

$\vec{U}$ = geostrophic wind velocity

$$\underset{\sim}{B}_a = \begin{bmatrix} \cos\alpha & -\sin\alpha \\ \sin\alpha & \cos\alpha \end{bmatrix}$$

α = counterclockwise drag angle

Water stress is represented by a quadratic drag law similar to that used in the atmospheric boundary layer. The stress on the lower surface of ice ($\vec{\tau}_w$) is a function of the ice velocity ($\vec{v}$) relative to $\vec{v}_g$:

$$\vec{\tau}_w = \rho_w C_w \left| \vec{v} - \vec{v}_g \right| \underset{\sim}{B} (\vec{v} - \vec{v}_g) \qquad (3)$$

where

ρ_w = water density

C_w = water drag coefficient = 5.5×10^{-3}

$$\underset{\sim}{B} = \begin{bmatrix} \cos(\pi-\beta) & -\sin(\pi-\beta) \\ \sin(\pi-\beta) & \cos(\pi-\beta) \end{bmatrix}$$

β = drag angle = 23°

Units are in the CGS system. The geostrophic flow is taken to be given by the long term observed values [Pritchard, et al, 1976].

The stress deformation constitutive law has been chosen as an elastic-plastic response. A plastic model possesses many of the properties thought to be desirable in describing the response of ice to wind stress. Specifically, it is able to simulate rapid variations which approximate discontinuous behavior in nearshore regions and simulate flow resembling a viscous material when a large enough load is applied. The constitutive law relates internal ice stress ($\bar{\bar{\sigma}}$) to the

large scale strain in the ice sheet. The ice is a stiff elastic material allowing elastic deformation of only about 0.1% before reaching a yield strength in compression and shear. Stresses are restricted to have no positive principal values because the material is densely fractured and will not support stress in any opening mode [Colony, 1976].

The thickness distribution measures the percentage of area covered by ice in each differential range of thickness within each element of the grid. A typical example is shown by the solid line in Figure 2. The thickness distribution determines the mass per unit area of the element as well as its mechanical properties. The thickness distribution is affected by both thermodynamic and mechanical processes. For example, the melting of a few centimeters off the top surface would shift the thickness distribution to the left, i.e., to the dashed line in Figure 2. During the winter, all but the very thickest ice grows thicker, shifting the curve to the right. When the element converges slightly, the thin ice is ridged into thick ice, causing the shape of the distribution to change as some thin ice disappears and a smaller increment of new thick ice is produced, as given by the dotted line in Figure 2. If the element diverges, open water forming between the floes would be shown in the distribution by a delta function at zero thickness. As time passes this open water would freeze into thin ice, moving the delta function to the right [Coon, et al, 1976]. In the AIDJEX model the growth rate is defined as the monthly climatological average [Pritchard and Colony, 1976].

One of the desirable properties of the AIDJEX model is the potential to express yield strength as a function of the thickness distribution. However, thus far, a satisfactory relationship has not been found and the yield strength is varied as a unique input parameter. The redistribution function and the energetics argument that enables strength to be determined from the thickness distribution will be reformulated as further work provides direction [Pritchard, et al, 1977].

The computational grid with manned camps and buoy locations for 15 May 1975 is shown in Figure 3. The grid was assembled according to the following rules: (1) The boundary may be a coastline or a dynamic boundary determined by the buoy positions, etc. Positions of the data buoys and the manned drifting stations were found using the Navy Navigational Satellite System and the buoy ring motion determines the boundary velocity conditions. This is the only boundary condition used in the model. (2) All interior cells must be quadrilaterals and all cells next to the boundary must be quadrilaterals or triangles. To minimize computer time, linear dimensions of all cells were made approximately equal. The stability of the difference scheme depends on the Courant restriction, $C\frac{\Delta t}{\Delta x} \leq \frac{1}{2}$, which means that the time step is proportional to the cell dimension, specifically the dimension of the smallest cell. The factor, C, is a function of ice strength; as ice strength increases the time step must decrease.

Initial conditions for a model run are contained on a computer file, magnetic tape or disk, which must be generated from a history of ice motion derived from buoy and manned camp positions. This file, called a DUMP file, contains positions of the grid points, initial velocities of grid cells, stress state, and ice thickness. Periodically during the model run this file is regenerated, providing a set of initial conditions to restart the run. Thus the model can be stopped and restarted several times during a lengthy run to allow checking of the solution or to rerun the problem and look at some event on a finer time scale. For example, if the solution were being saved for plotting every four hours, it might be desirable to return and look at the solution every twenty minutes for some four-hour period. The DUMP file also serves as the data source for plotting two-dimensional fields.

One additional output from the model is a time history of data from 20 selected nodes. Saving the solution at only a fraction of the nodes enables one to plot the solution densely in time, enabling high frequencies to be seen without using excessive amounts of storage [Don Thomas, AIDJEX, personal communication].

The parts of the model, i.e., the momentum equation and the constitutive laws are solved simultaneously. Detailed equations and methods of solution are given by Pritchard and Colony [1976].

IV. EVALUATION OF FNWC SEA-LEVEL PRESSURE FIELD AND GEOSTROPHIC WINDS

Fleet Numerical Weather Central (FNWC), located in Monterey, California, is responsible for providing all numerical environmental forecasts in support of Naval operations. FNWC is linked to the National Meteorological Center (NMC), the Air Force Automated Weather Network (AWN), and in addition receives observations from Navy units throughout the world [U. S. Naval Weather Service, 1975]. The numerical products produced at FNWC include sea-level pressure, upper-air analyses and prognoses, marine layer winds, sea-surface temperature, and many others produced on a polar stereographic projection from data analyzed on a rectangular grid. Most fields are resolved on a 63 x 63 point Northern Hemispheric grid but other grids are used for some products. Atmospheric prognoses (forecasts) are made twice a day at 0000GMT and 1200GMT for each 12-hour period out to 72 hours. Many computational algorithms are used to generate the numerical products but one of the most important is that which blends available information to formulate the best possible sea-level pressure field. This is known as the Fields by Information Blending (FIB) technique.

A. DESCRIPTION OF THE FIELDS BY INFORMATION BLENDING (FIB) TECHNIQUE

At FNWC, sea-level pressure is analyzed to a 125 x 125 polar stereographic projection hemispheric grid (grid spacing

190 km at 60°N) using the FIB technique [Holl and Mendenhall, 1972]. While analyzed on a 125 x 125 grid the resultant field is archived on a 63 x 63 grid which has a 381-km spacing at 60°N.

The FIB generation of the sea-level pressure analysis is illustrated in Figure 4. The basic steps in the FIB analysis technique are:

1. The 6-hour old analysis is extrapolated to the present analysis time, assembled at each grid point and combined with the 6- or 12-hour old prognosis to produce a first guess field.
2. New wind and pressure reports are assembled, rejecting errors and weighting individual values according to their reliability.
3. Available information fields are blended into a modified first guess field.
4. Fields of sea-level pressure, sea-level pressure gradient and the Laplacian of the pressure field are analyzed and blended to obtain the best fit field.
5. New reliability weights are determined.
6. A new gross error check and reevaluation of data is made.
7. Assembly, blending and resultant weight operations are recycled.
8. The final best-fit pressure field is output.

Since the resulting pressure field is a blend of available information, in the absence of observations the analysis

will be largely based on the previous prognosis. However, the quality of the prognosis is dependent upon the accuracy of the previous analysis. Thus, in data sparse areas such as the Arctic, the analysis is prone to greater error than a data rich area.

B. SEA-LEVEL PRESSURE EVALUATION METHOD

Evaluation of FNWC's atmospheric sea-level pressure analysis was performed by using AIDJEX sea-level pressure observations as a standard. Twenty-day files of sea-level pressure observations and geostrophic wind analyses were obtained from AIDJEX on magnetic tape. The period from 1 May through 19 July 1975 (AIDJEX days 121-200, four 20-day intervals) was selected for detailed evaluation.[1] AIDJEX data represent high density, high quality observations from several manned camps and remote buoy stations whose positions on 18 May 1975 are shown in Figure 5. The FNWC sea-level pressure analysis for this time is shown in Figure 6.

FNWC's 6-hourly analyses and 12-hourly prognoses of sea-level pressure fields were interpolated to each AIDJEX observation station. The RMS pressure difference (where pressure difference is $\Delta P = P_{FNWC} - P_{AIDJEX}$) at all AIDJEX stations in each 20-day interval was calculated for the analysis, 24-, 48-, and 72-hour prognoses, and the results are summarized in Figure 7. The RMS pressure difference (a measure of the

---

[1]AIDJEX days are Julian days measured from 1 Jan 1975 and continue to be consecutively numbered into 1976. Thus 2 Jan 1976 is AIDJEX day 366.

quality of the product) increases from 2.3 mb in the first interval (A, 1-20 May) to 3.4 mb in the last interval (D, 30 June to 19 July). For the prognostic times the error increases by about 0.6 mb for the first 24-hour period and thereafter by about 2 mb for each 24-hour projection. For some reason the second and third time intervals (B, 21 May to 9 June and C, 10-29 June) show an increase in quality over the first interval. However, the quality is always poorest in the final interval which is the summer period.

An explanation for the larger RMS ΔP values in the fourth time interval is found in Figure 8 which shows a time series of atmospheric sea-level pressure at the AIDJEX main camp over the entire 80-day period. The greatest variability of the pressure is in the fourth period implying an increased synoptic activity level. This increased activity combined with lack of observations probably accounts for the decreased quality.

An attempt was made to determine if and when observations from AIDJEX were included in the FNWC analysis. A search was made of FNWC archives for any reports submitted by AIDJEX. A total of 95 AIDJEX reports were found in the archives, reported only from the main AIDJEX camp. However, due to the nature of the archiving system late reports (up to 24 hours) are archived and it is not possible to determine if any particular report was included in the analysis. RMS ΔP for analyses corresponding to archived reports is shown by the line marked R on Figure 7. A careful examination of Figure 8 reveals the effect of the inclusion of an AIDJEX pressure

observation in the FNWC analysis. Time of archived AIDJEX observations are indicated by "tick" marks near the lower edge of the graph. The circled areas illustrate a few times corresponding to archived observations when the analysis has made a sharp change in trend to become coincident with the value of the observations. It can be inferred that the AIDJEX reports did reduce errors in the FNWC analysis by 0.7 mb on the average and that any observations from the central Arctic will probably result in an improved analysis.

Walsh [1977] has calculated the RMS height errors for the 1000 mb height forecasts of the NMC primitive equation model at 16 grid points covering roughly the same area as the AIDJEX observation stations. His technique involved finding the height error of the 24-, 48-, and 72-hour forecasts using the verifying analysis as a standard. When converted to millibars (8 m = 1 mb) these errors range from 2-3 mb at 24 hours to 5-6 mb at 72 hours. This technique of using the verifying analysis vice observations as a standard was applied to the FNWC data, again interpolated to the same AIDJEX station locations. The RMS ΔP increases from 2.5 mb at 24 hours to 6.5 mb at 72 hours. These are comparable to the results found by Walsh. However, they show a marked improvement over the use of observations as a standard, the improvement ranging from 1.0 at 24 hours to .3 mb at 72 hours. This suggests that the use of the verifying analysis as a standard for forecast evaluation yields optimistic results primarily because the analysis is largely based on the previous prognosis in the Arctic area.

Sufficient pressure data were available from AIDJEX to evaluate FNWC analyses from 1 May 1975 through 24 April 1976. The results of the evaluation are shown in Figure 9. $\overline{\Delta P}$ began at about 0.3 mb (higher pressure than actually existed) and continued increasing into the summer until the end of August when the value reached 2.7 mb. It decreased as fall approached becoming negative in mid-October, and generally remained negative throughout the winter, becoming positive the following March.

The RMS ΔP remained high throughout the summer, decreased slightly in the fall and remained lower than the summer values throughout the winter. The sharp increase in March can be attributed to increased synoptic activity. An evaluation of whether these fluctuations of RMS ΔP and $\overline{\Delta P}$ follow an annual cycle will become possible when a longer record of complete observations in the Arctic become available.

C. METHOD OF EVALUATION OF GEOSTROPHIC WINDS

An evaluation of FNWC geostrophic winds was performed to determine their suitability for air stress computation. In the AIDJEX model and probably any other operational model the wind stress is determined from the geostrophic wind. Therefore, the quality of the sea-level pressure field is an important consideration. The AIDJEX sea-level pressure field is expressed by a least squares polynomial fit to all data points [AIDJEX, 1976]. However, geostrophic winds are dependent on the pressure gradient rather than the actual

pressure values at any point. Geostrophic winds, as obtained from AIDJEX, are found by differentiating the polynomial expression along grid directions at each observation station.

To obtain FNWC geostrophic winds, a fourth order finite differencing technique was applied to the FNWC grid point sea-level pressure value to determine the pressure gradient components. FNWC geostrophic wind components were then interpolated to AIDJEX observation stations and compared with AIDJEX geostrophic winds. The RMS wind speed and direction differences were calculated and the results are summarized in Figure 10 where wind speed differences have been normalized by the AIDJEX value. Aggregate results of all four evaluation periods are marked by *G which shows increased differences as the forecast period increases. In particular the direction differences increase from about 50° to 75° from analysis to the 72-hour forecast, respectively. The fractional speed errors show an increase from 0.65 to 1.35 for the same periods.

If only wind speeds in excess of 5 m/sec are considered, the RMS differences decrease significantly, and only a slight increase from 0.4 to 0.5 is found as the forecast period lengthens. These values are of particular interest since the air stress is taken as proportional to the square of wind speed and the higher wind speeds will be of greater importance in determining ice drift. There is a relative minimum in both direction and speed differences in the 21 May to 9 June time period which corresponds to the reduced RMS pressure error in this time frame. However, for some reason the direction and speed difference for period C do not similarly correspond

with the relatively low RMS pressure errors for that time frame.

D. SIMULATION RESULTS

To more completely evaluate the usefulness of the FNWC sea-level pressure field in driving an ice dynamics model, a simulation using the AIDJEX model was made. The AIDJEX model was programmed on the FNWC 6500 computer to simulate ice movement during the period 0300GMT 15 May to 1200GMT 25 May 1975. Air stress derived from the FNWC sea-level pressure analysis field was used in the simulation while all other input parameters and boundary conditions were specified as those used by AIDJEX. The air stress field was computed using equation (2) and assembled in a form compatible with the AIDJEX model using the following values of air density (ρ_a), drag coefficient (C_D) and turning angle (α):

$$\rho_a = 0.00135 \text{ gm/cm}^3$$
$$C_D = 11 \times 10^{-4}$$
$$\alpha = 20°$$

C_D and α are the same values used in AIDJEX model simulations [Eric Levitt, AIDJEX, personal communication].

Figures 11 and 12 show time series plots of both FNWC and AIDJEX computer air stress magnitude and direction at two grid points. It is clear that the FNWC air stress is smaller than the AIDJEX air stress, in particular for the important time periods days 135-136 and 137-140, when there is a high air stress. At node 7,7, which corresponds to the main AIDJEX camp, during day 135 the FNWC air stress is 20% of

AIDJEX values. From day 137 to 140 the FNWC air stress is in general much less than AIDJEX. The values at node 3,7 follow a similar pattern, the FNWC stress being a small fraction of the AIDJEX value for the first day, and the FNWC stress generally retaining the trends of the AIDJEX stress, but at reduced levels. In addition to the magnitude differences there are direction differences of up to 150°, however, these are generally limited to the light wind conditions. The direction differences for the critically high stress period 137-140 are small, i.e., generally less than 30°.

Figures 13 and 14 show vector field plots of air stress at 1200GMT 18 May for the AIDJEX and FNWC model runs, respectively. The AIDJEX plot shows considerable spatial variation, with an area of high stress over the southern portion of the region. The FNWC stress field plot shows less spatial variation and significantly smaller air stress over the northeastern portion of the region.

The trajectories computed using FNWC and AIDJEX stress fields for the main AIDJEX camp are shown in Figure 15. The total displacements of the FNWC projected movement is comparable to the AIDJEX movement with only a 3 km difference in the final positions. In addition to the comparable total displacement, the small-scale features of the AIDJEX movement are retained in the FNWC movement. Figure 15 also includes the actual movement of the AIDJEX main camp as calculated from AIDJEX measured positions [Thorndike and Cheung, 1977]. It is clear that neither AIDJEX nor FNWC followed the movement exactly. During the first several days the FNWC movement

more closely resembles the true motion, while in the final positions the AIDJEX simulation is closer, namely 3 km versus 4.5 km.

A more detailed analysis is possible by looking at the x- and y-position time series for the main camp. Figure 16 shows the x- and y-position time series relative to the AIDJEX coordinate system [Thorndike and Chueng, 1977]. It is evident that the error in the y-position was accumulated largely in the first two days. Referring back to Figure 11, the FNWC air stress is only about 0.3 dynes/cm^2 compared to 1.5 dynes/cm^2 for AIDJEX. This low FNWC value is the cause of most of the difference in the final position.

The relative motion of two or more stations is important for those processes such as deformation which depend on differential motion. The trajectory of node 3,7, located in the left hand portion of the grid, is shown in Figure 17. It has a larger scale of motion than the main camp and the final error is in the opposite direction, being about 3 km in the negative y direction. This quantitatively implies a larger deformation difference between the two stations than the absolute motion difference of either single station. Node 3,7 had no position measurements to allow checking of the results of the simulations.

Figure 18 shows the x- and y-position time series for node 3,7. Unlike node 7,7, whose error was accumulated largely in the first day, this node accumulated its error in the 138-139 day time frame. For node 3,7 the error steadily increases from day 137-139.5, this time period corresponding

to the maximum difference in air stress between the two runs (Figure 11).

Figure 19 is a vector plot of the ice velocity field for the AIDJEX simulation at 1200GMT 18 May. Recalling that the boundary velocity is specified, it is evident that the discontinuities in the velocity field along the southwest and northeast boundaries represent errors in the calculated velocities. Figure 20 is a vector plot of the stress divergence field at the same time showing relatively large stress divergence forces along the south and northeast boundaries. The turning of the vector along the south boundary implies that the stress is an artifact of the discontinuous velocity field and probably has the effect of directing the field velocity into agreement with the boundary velocity.

Figure 21 is a vector plot of the velocity field for the FNWC simulation at 1200GMT 18 May. The velocity discontinuity along the northeast boundary is similar to AIDJEX but there is no apparent discontinuity along the south boundary. The regular pattern of the stress divergence shown in Figure 22 appears to be a more natural occurrence than does the AIDJEX stress divergence field, implying that at least for this one time the FNWC simulation is a better representation than the AIDJEX simulation of the actual ice dynamics.

The relationship of the two computed velocities is shown in Figure 23. The only large differences in the velocities are for days 135 and 137. These correspond to the large differences in air stress values. The remaining time period shows a high correlation between the two data sets, an even

higher correlation than would seem to be supported by the significant differences in the air stress alone. The reasons for this high correlation can be attributed to the influences of the boundary velocity condition. The ice is largely affected by internal ice stress during the light wind conditions and is primarily driven by the boundary velocity inputs. This is amply illustrated in Figures 24 through 27 where the FNWC and AIDJEX air stress fields are radically different yet the velocity fields are nearly identical. The model is being run by the boundary at this time.

V. CONCLUSIONS

A comparison of FNWC sea-level pressure analyses and prognoses with observations made by AIDJEX during the spring and summer of 1975 shows:

1. A RMS error of approximately 3 mb for the analysis time increasing to approximately 7 mb at 72 hours.
2. The RMS error is highest during the summer months, increasing from 2.3 mb in May to 3.8 mb in July.

Comparing the FNWC sea-level pressure analyses and AIDJEX observations for the 360-day period from 1 May 1975 to 24 April 1976 shows:

1. The RMS error remains relatively high throughout the summer, decreases into fall and winter with a sharp rise in February.
2. The average ΔP increases to a maximum of 1.7 mb in August, becoming negative in October reaching a minimum of -1.0 mb in November, and then becomes positive again in late winter.

Of particular note is the fact that the inclusion of just one observation for the AIDJEX ocean improves the pressure analysis by nearly 1 mb.

A comparison of FNWC generated geostrophic winds with AIDJEX generated geostrophic wind reveals:

1. The normalized RMS speed difference for all wind speeds increases from 0.65 to 1.35 from analysis to the 72-hour prognosis.

2. Considering only wind speeds greater than 5 m/sec, the normalized RMS speed difference is lower and increases from 0.4 to 0.5 from analysis to 72-hour prognosis.

The movement of two AIDJEX grid nodes using FNWC sea-level pressure fields to derive wind stress in a ten-day simulation closely approximates the movement calculated by AIDJEX. Final position errors compared to measured positions of the main camp were 4.5 km for the FNWC simulation versus 3 km for the AIDJEX simulation. The other node had a difference of about 3 km between AIDJEX and FNWC simulations. The majority if not all the final position error was accumulated during periods of high air stress when FNWC air stress was 20% to 80% of the AIDJEX value.

During periods of low wind stress the AIDJEX model is largely driven by the boundary velocity conditions as evidenced by the high correlation of AIDJEX and FNWC calculated velocities during these periods.

The performance of the AIDJEX model is highly dependent on the accurate specification of the boundary velocities. Any attempt to use the model as a predictive tool will be limited by the use of the boundary conditions. The present method is not realistic for forecasting and must be replaced by some form of wind driven boundary. A significant degradation of the performance of the model can be expected to result from the use of a wind driven boundary.

Another limitation of the model's use for forecasting is the amounts of computer time required for a simulation. A 72-hour simulation required about 1.5 hours computer time on a CDC 6500 computer. This is fully one-fourth the time required to generate a 72-hour 7-level primitive equation meteorological prognosis for the entire Northern Hemisphere.

The important ice thickness distribution was not investigated in the simulation because it was deleted from the model for reasons relating to its contribution to the ice strength calculations. However, it may be included later if one desires it for other than ice strength considerations.

VI. RECOMMENDATIONS

It is recommended that the Navy continue work on operational ice dynamics models. Specific areas of investigation should include a formulation of boundary conditions which are compatible with a forecasting vice hindcasting scheme, preparation of a model which works well in the summer shipping season, and incorporation and evaluation of an ice thickness distribution technique which is independent of ice strength calculations.

Furthermore, every effort should be made to provide synoptic sea-level pressure and air temperature observations from the central Arctic. The satellite telemetry buoys developed and used in conjunction with the AIDJEX field experiment offer one of the simplest and most direct means of improving the environmental forecasts in the Arctic. Without the real time availability of these observations, good predictions of ice conditions encompassing all Navy requirements will remain an impossibility.

APPENDIX A FIGURES

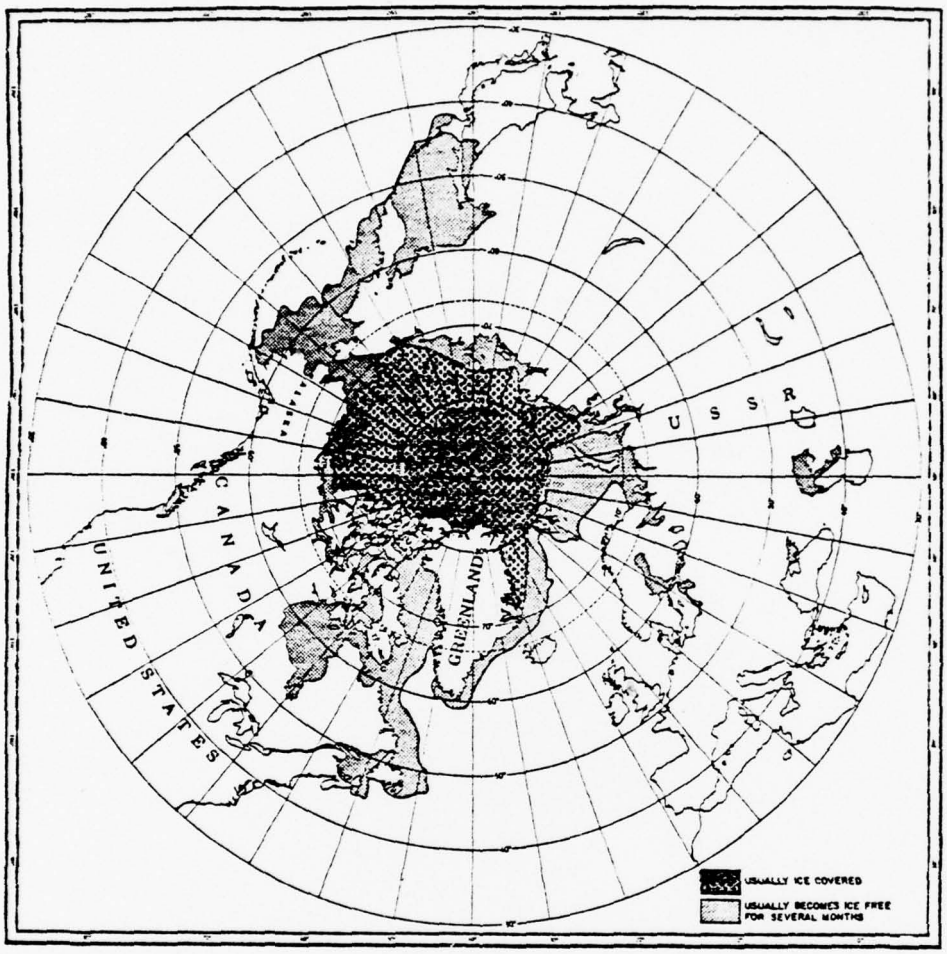


Figure 1. Extent of sea ice in the Northern Hemisphere. [Sater, Ronhovde, and Van Allen, 1971]

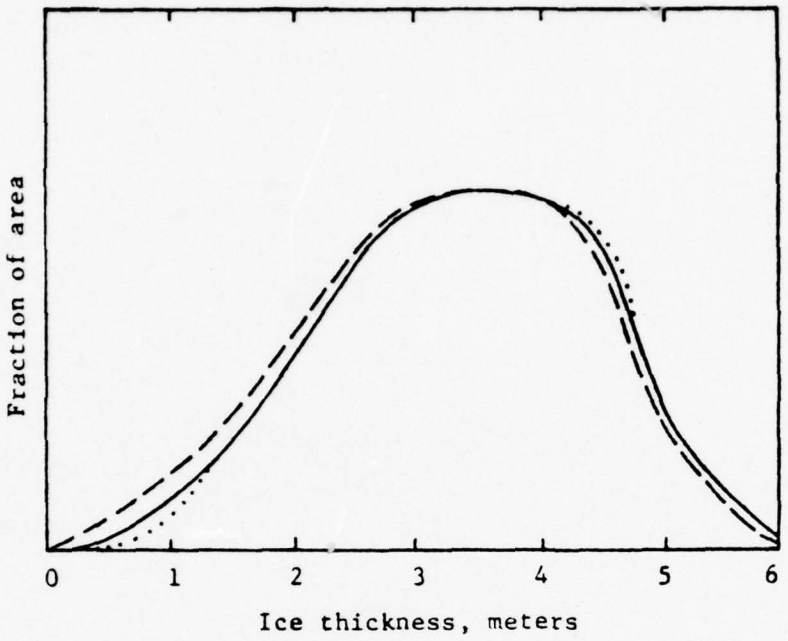


Figure 2. A representative thickness distribution undergoing changes described in the text. [Coon, et al, 1976]

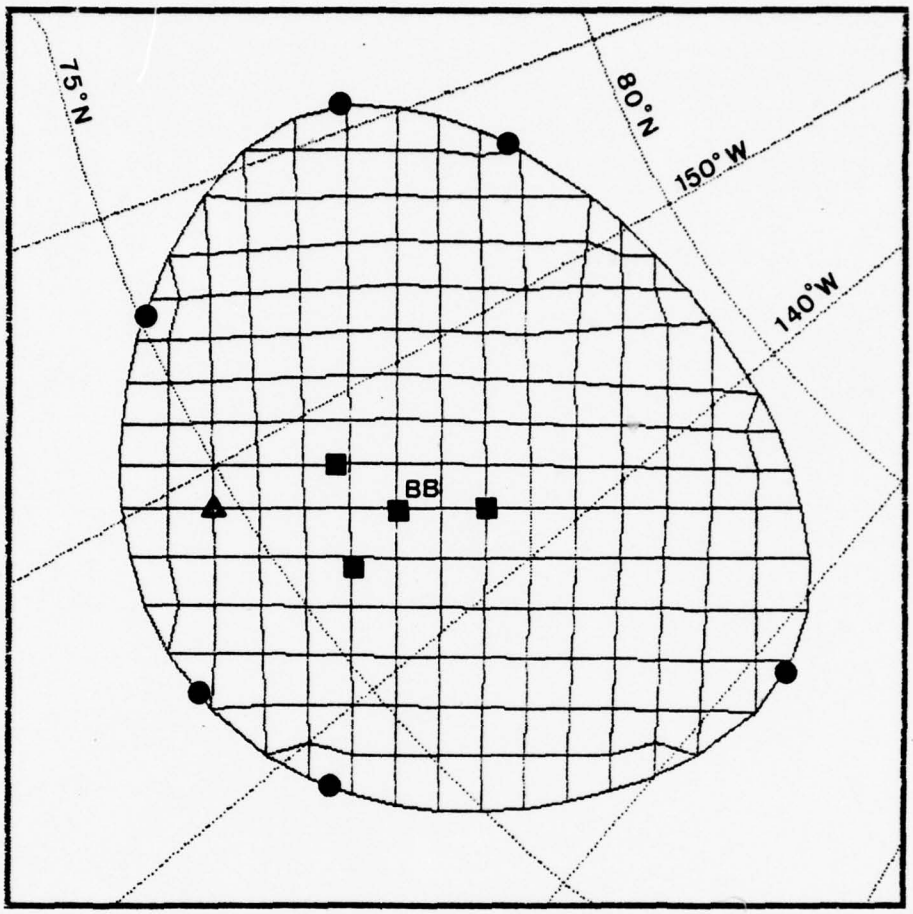


Figure 3. The AIDJEX computational grid at 0300GMT 15 May 1975. Observation stations are marked as: remote buoys (●), manned camps (■), main AIDJEX camp (node 7,7) (■ BB). Node 3,7 is marked as (▲). Irregular configuration of the grid is a result of applying the rules for generating the grid as described in the text.

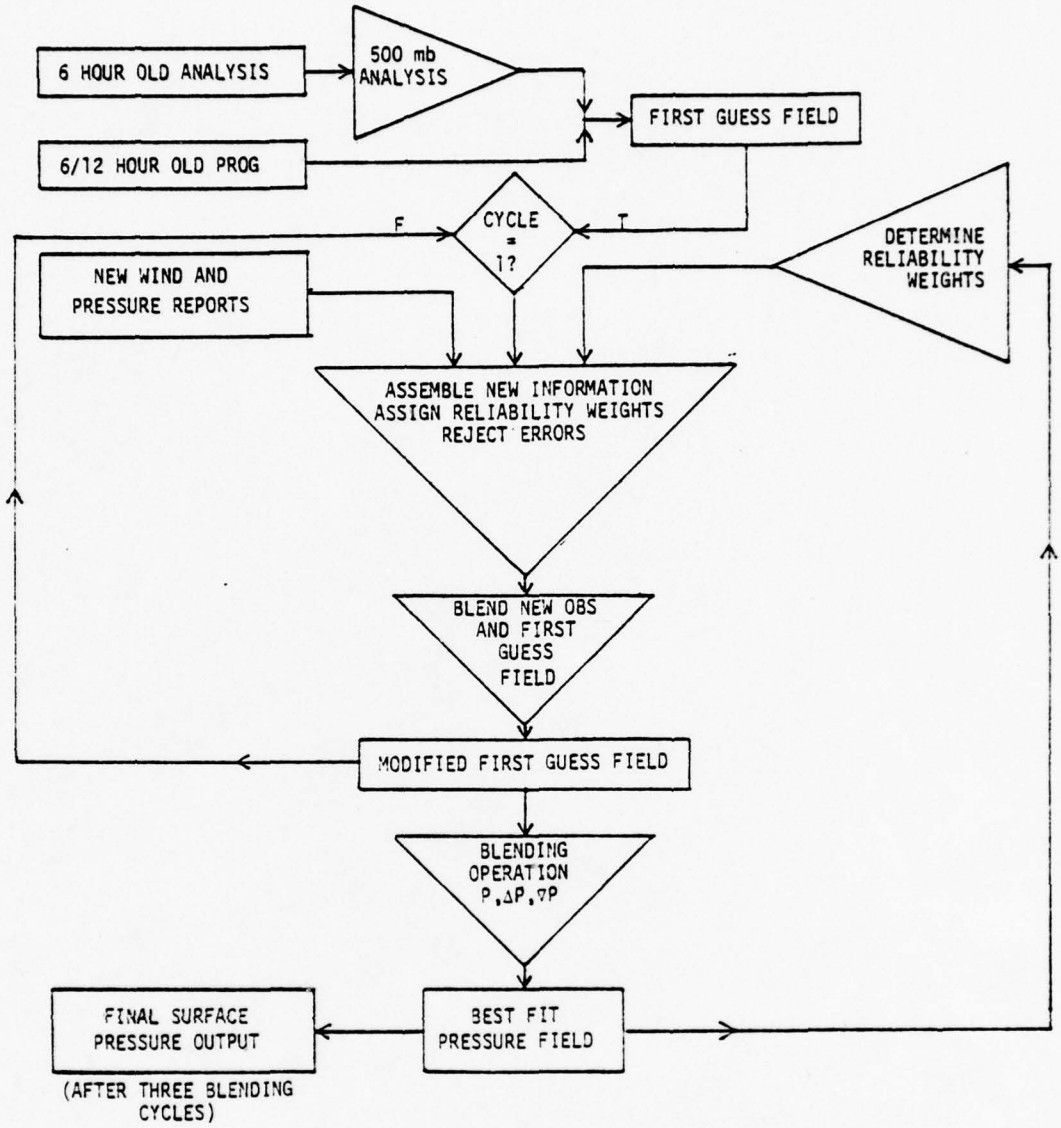


Figure 4. Simplified flow diagram of FNWC's Fields by Information Blending (FIB) Sea-Level Pressure analysis technique.

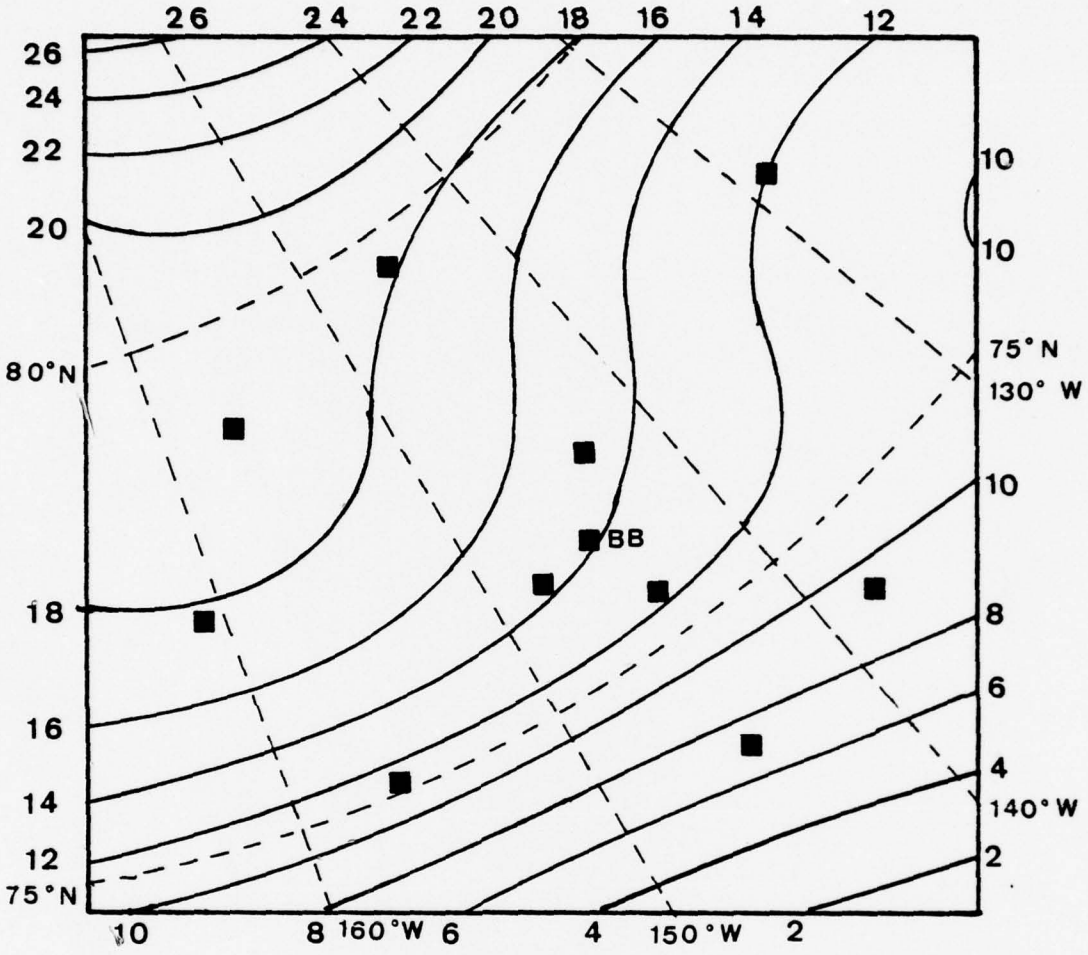


Figure 5. AIDJEX sea-level pressure analysis for 1200GMT 18 May 1975. Values are sea-level pressure minus 1000 mb. AIDJEX observation stations are marked by (■). Station marked BB is the location of AIDJEX main camp (Big Bear).

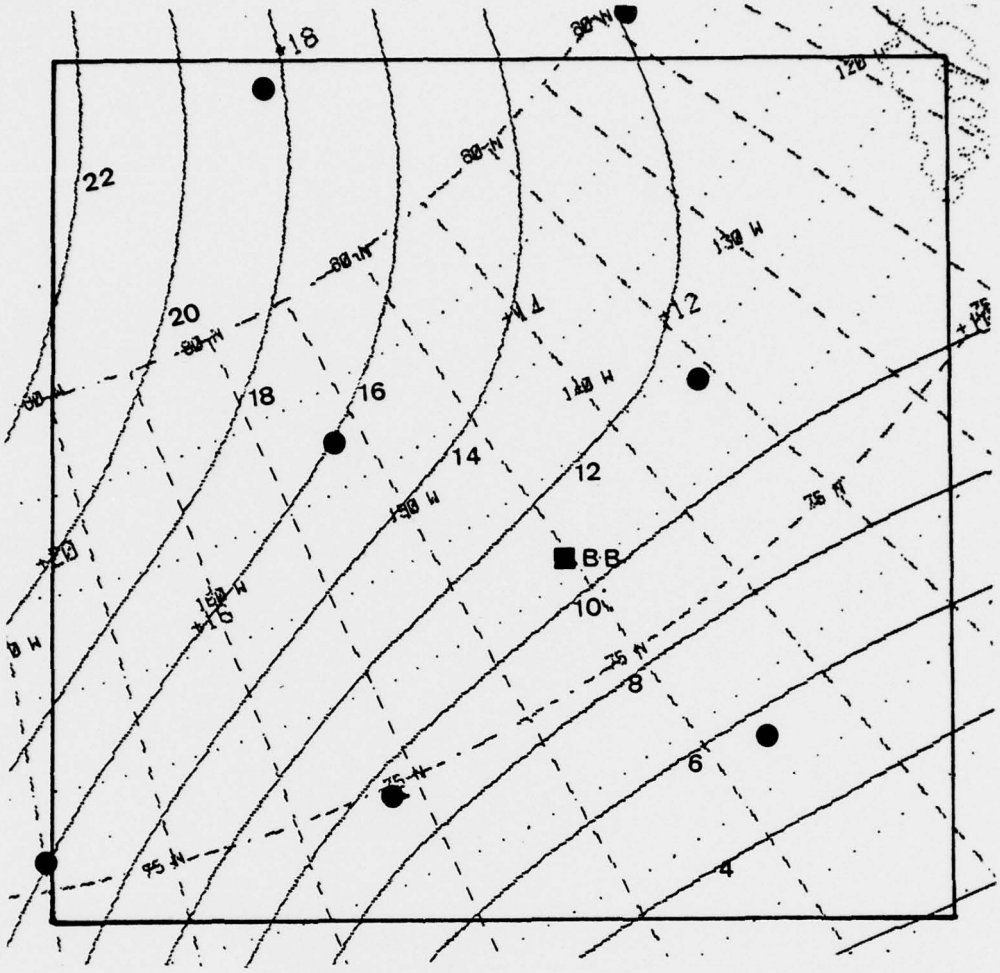


Figure 6. FNWC sea-level pressure analysis for 1200GMT 18 May 1975. 63x63 grid points are marked (●). Station marked (■ BB) is location of AIDJEX main camp. Values are sea-level pressure minus 1000 mb.

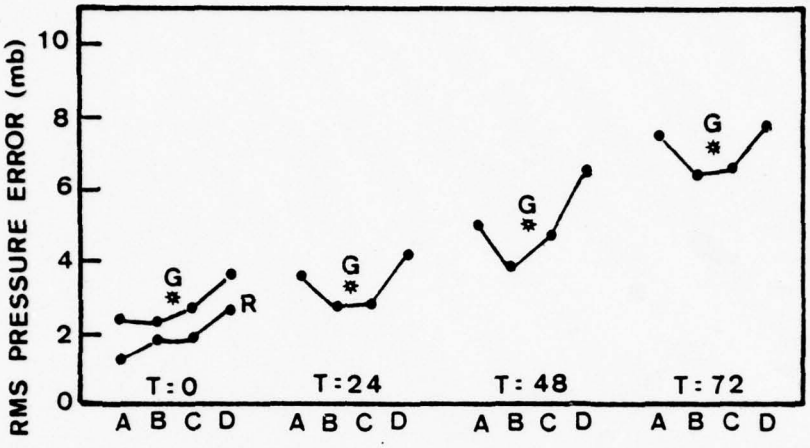


Figure 7. RMS pressure error for FNWC sea-level pressure analysis and prognoses at all AIDJEX stations. Analysis time is T=0, T=24 is 24 hour prognosis, T=48 is 48 hour prognosis, T=72 is 72 hour prognosis. Dates are shown by A, 1 May to 20 May; B, 21 May to 9 June; C, 10 June to 29 June; and D, 30 June to 19 July. Points marked *G are aggregate errors for all four time periods. Line marked R is RMS error for only those analysis times corresponding to FNWC-archived AIDJEX observations.

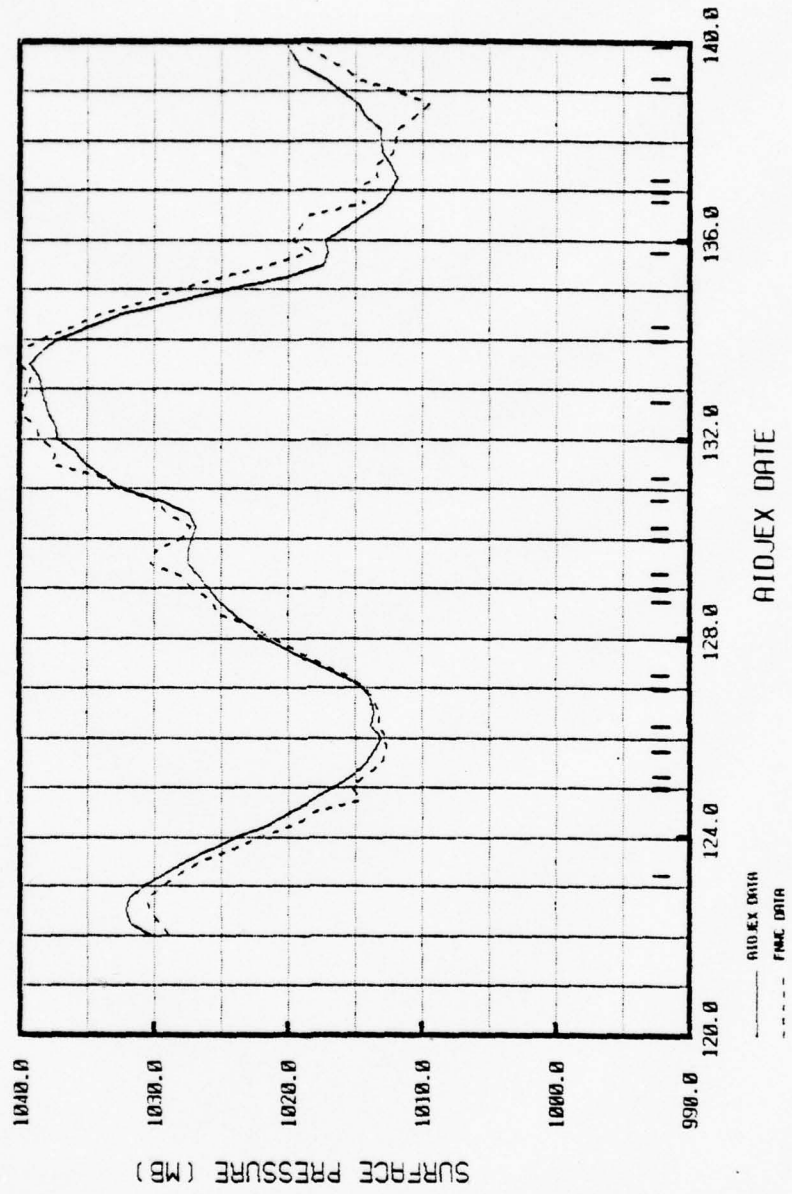


Figure 8a. Time series of AIDJEX sea-level pressure observations (solid line) and FNWC analysis (dashed line) for AIDJEX main camp for period 1 May to 20 May 1975. "Tick" marks indicate analysis times corresponding to FNWC-archived AIDJEX observations.

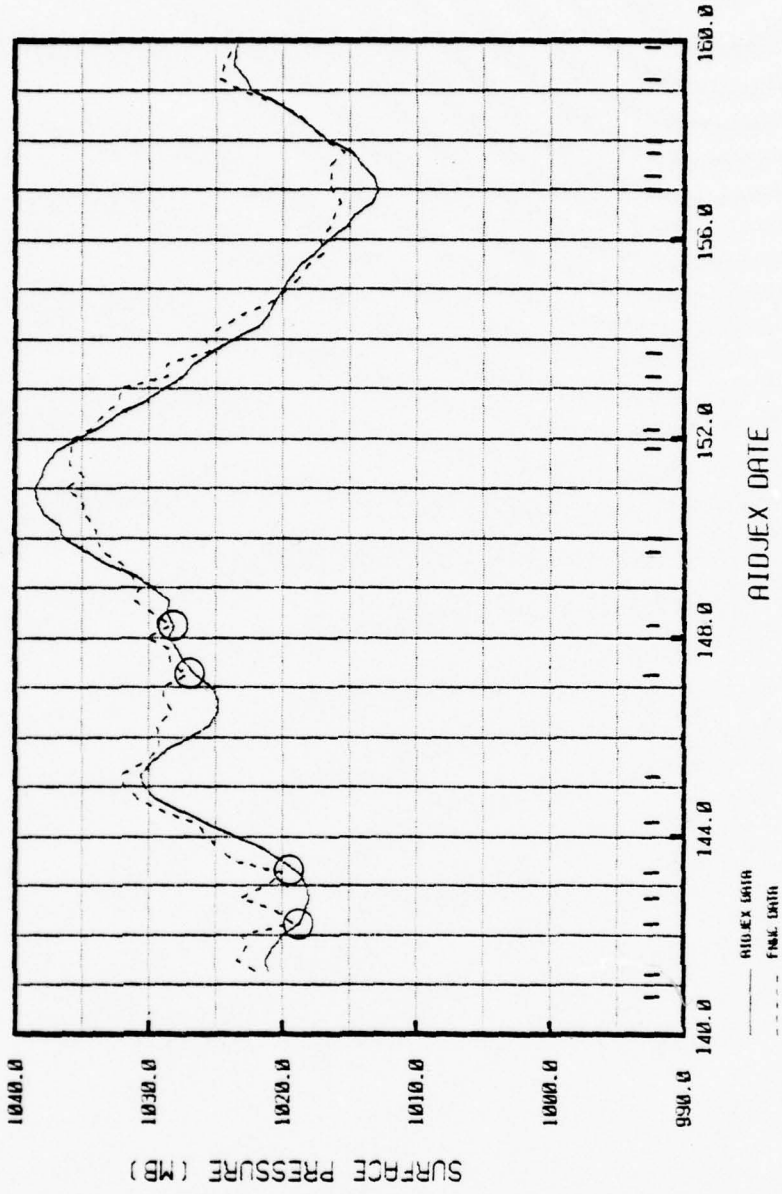


Figure 8b. Time series from 21 May to 9 June 1975. Circled portions indicate FNWC-archived AIDJEX observations which obviously had the effect of bringing the FNWC analysis to the AIDJEX observed values.

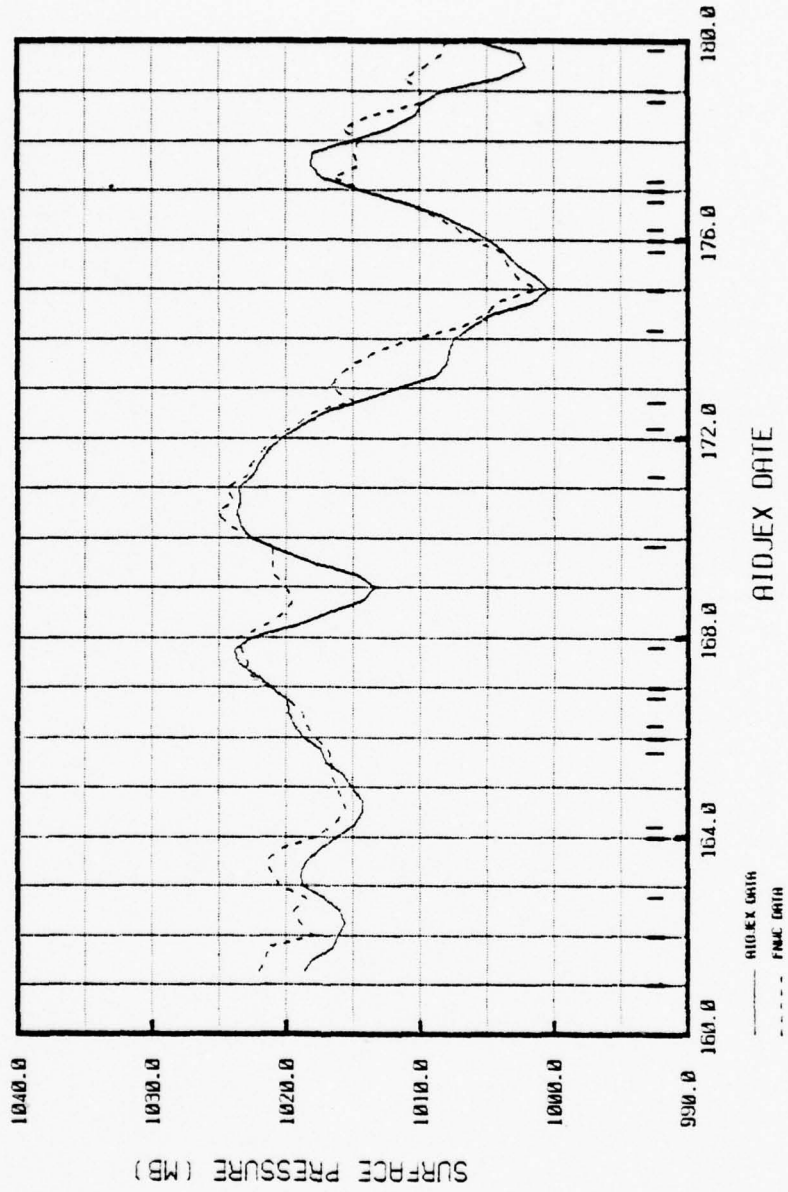


Figure 8c. Pressure time series from 10 June to 29 June 1975.

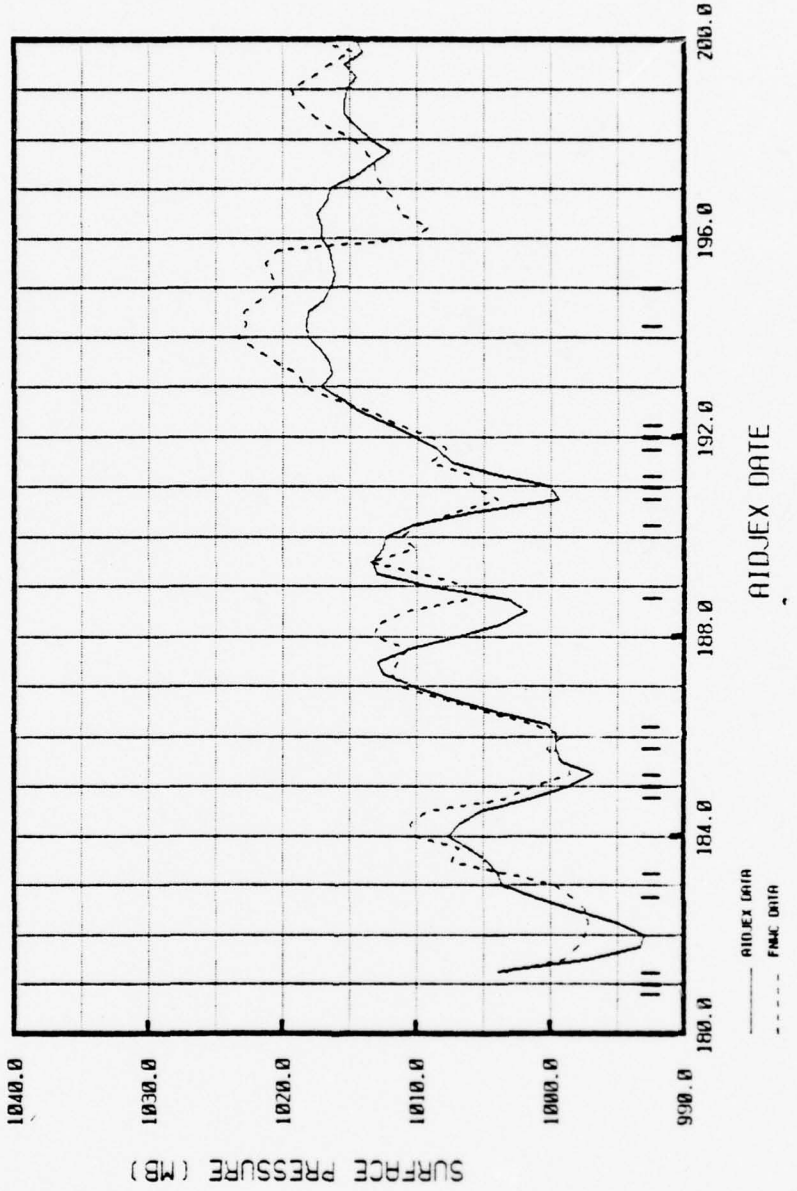


Figure 8d. Pressure time series from 30 June to 19 July 1975.

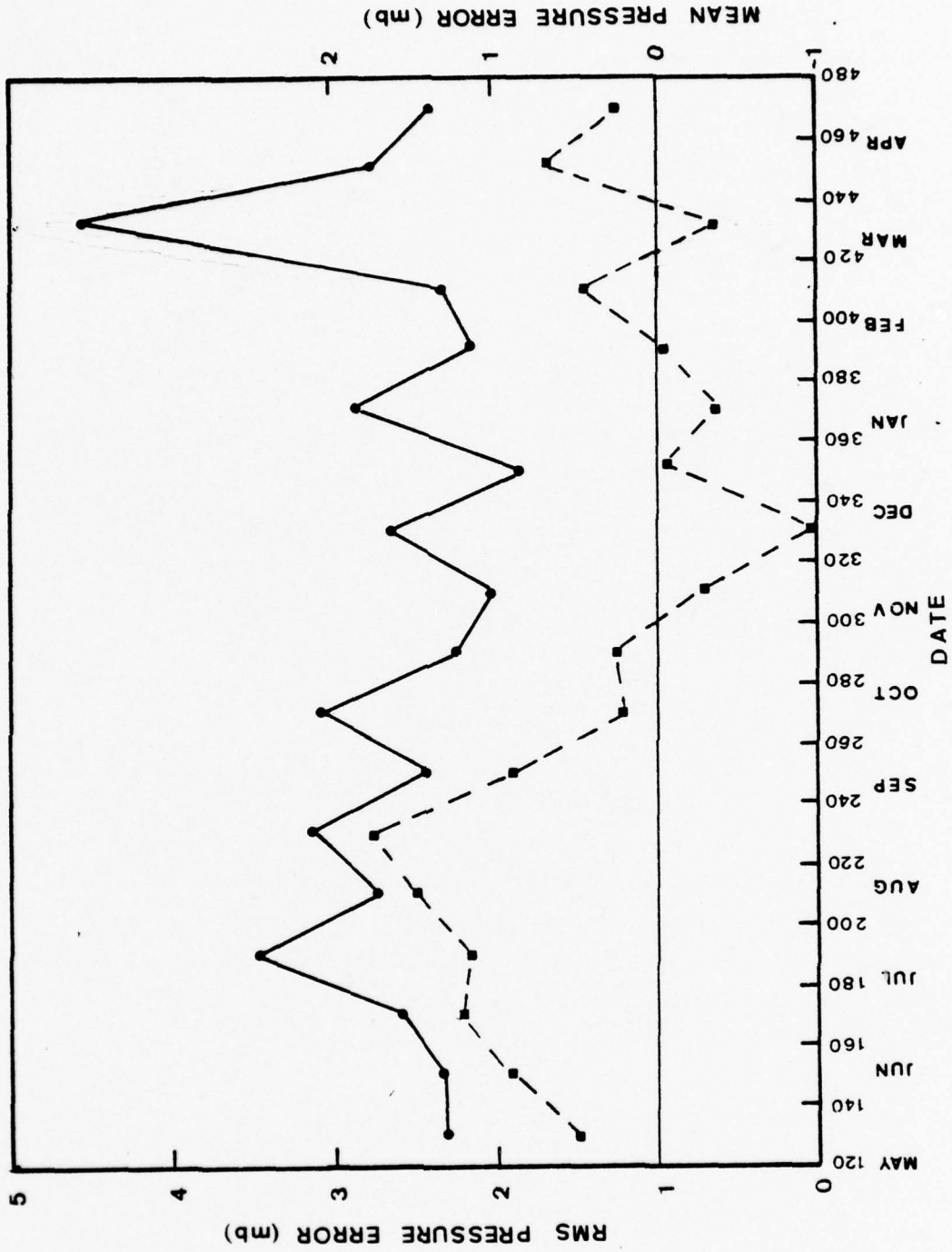


Figure 9. RMS pressure errors and mean pressure errors for FNWC analysis at all AIDJEX stations for the period 1 May 1975 to 24 April 1976. Dates indicated are AIDJEX days. Each point represents 20-day average value. The beginning of each month is indicated. RMS error is shown by a solid line, mean error by a dashed line.

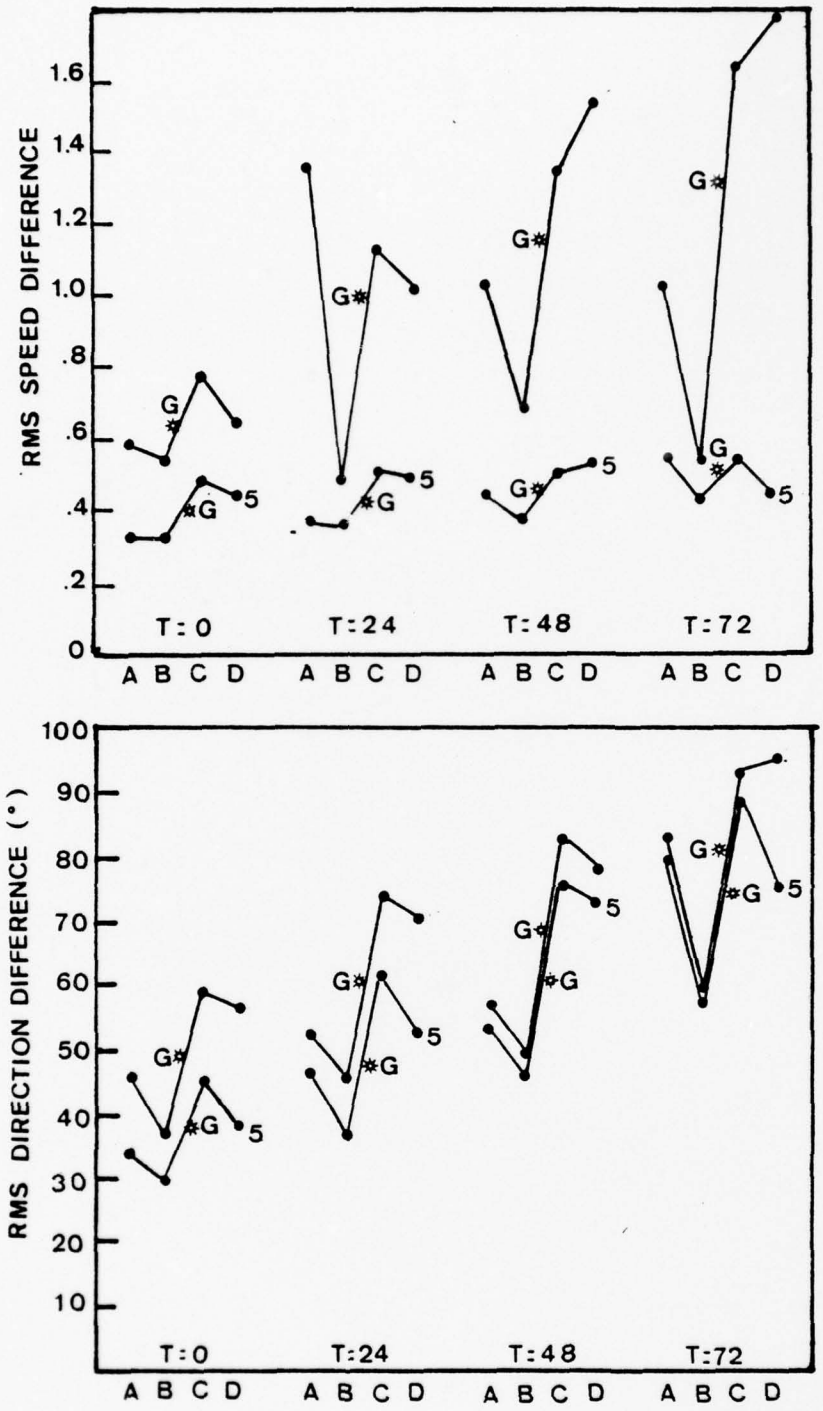


Figure 10. RMS wind speed and direction difference between AIDJEX analyzed and FNWC analyzed and prognosticated winds. Lines marked 5 are differences for only those wind speeds greater than 5 m/sec. Points marked *G are aggregate differences for all four time periods. Time periods are A, 1 May to 20 May; B, 21 May to 9 June; C, 10 June to 29 June; and D, 30 June to 19 July.

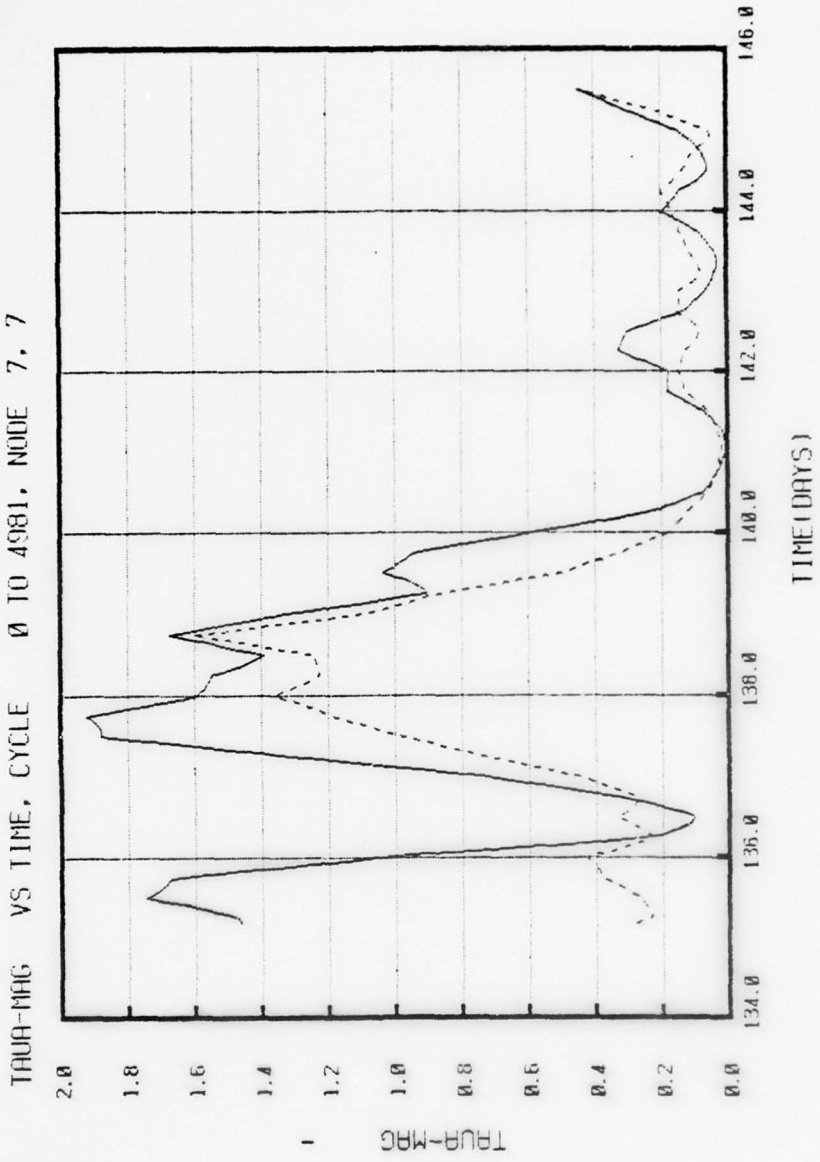


Figure 11a. Computed air stress magnitude (TAUA-MAG) from AIDJEX field (solid line) and FNWC field (dashed line) at AIDJEX main camp for days 15 to 25 May 1975. Units are dynes/cm^2.

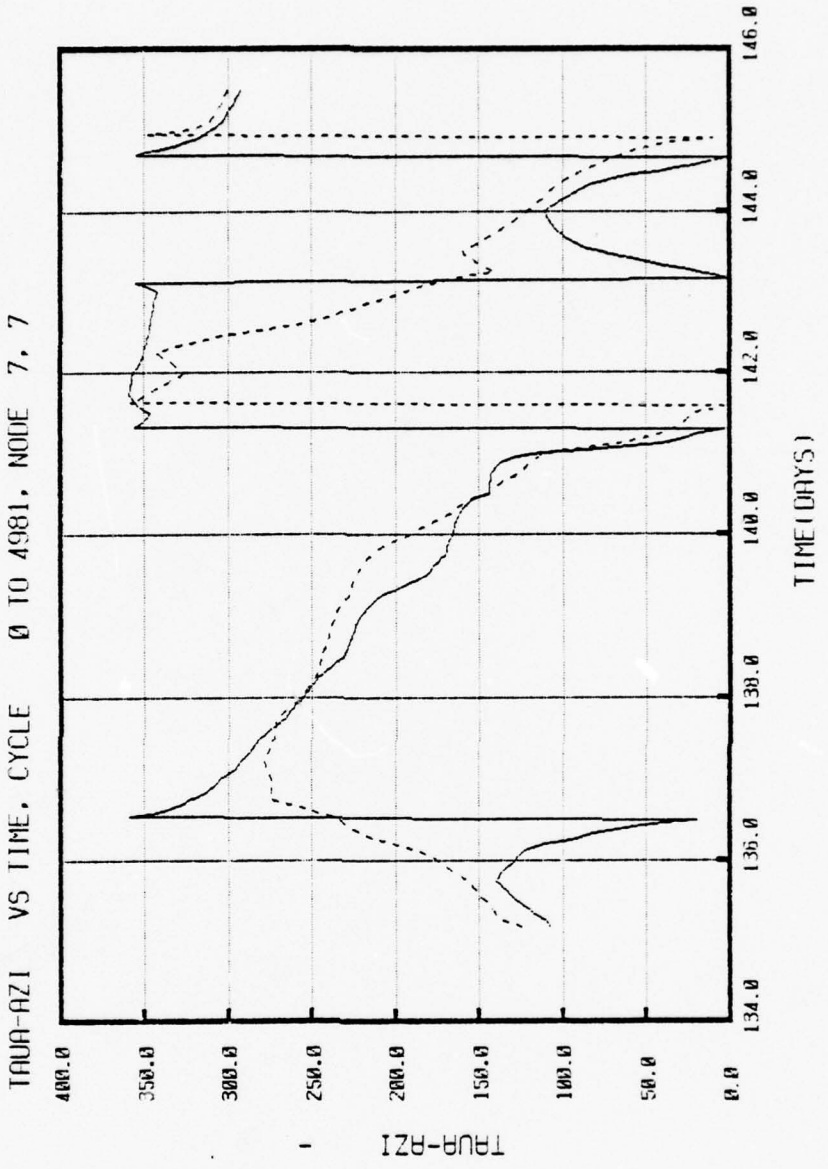


Figure 11b. Computed air stress direction (TAUA-AZI) from AIDJEX field (solid line) and FNWC field (dashed line) at AIDJEX main camp for days 15 to 25 May 1975. Units are degrees true.

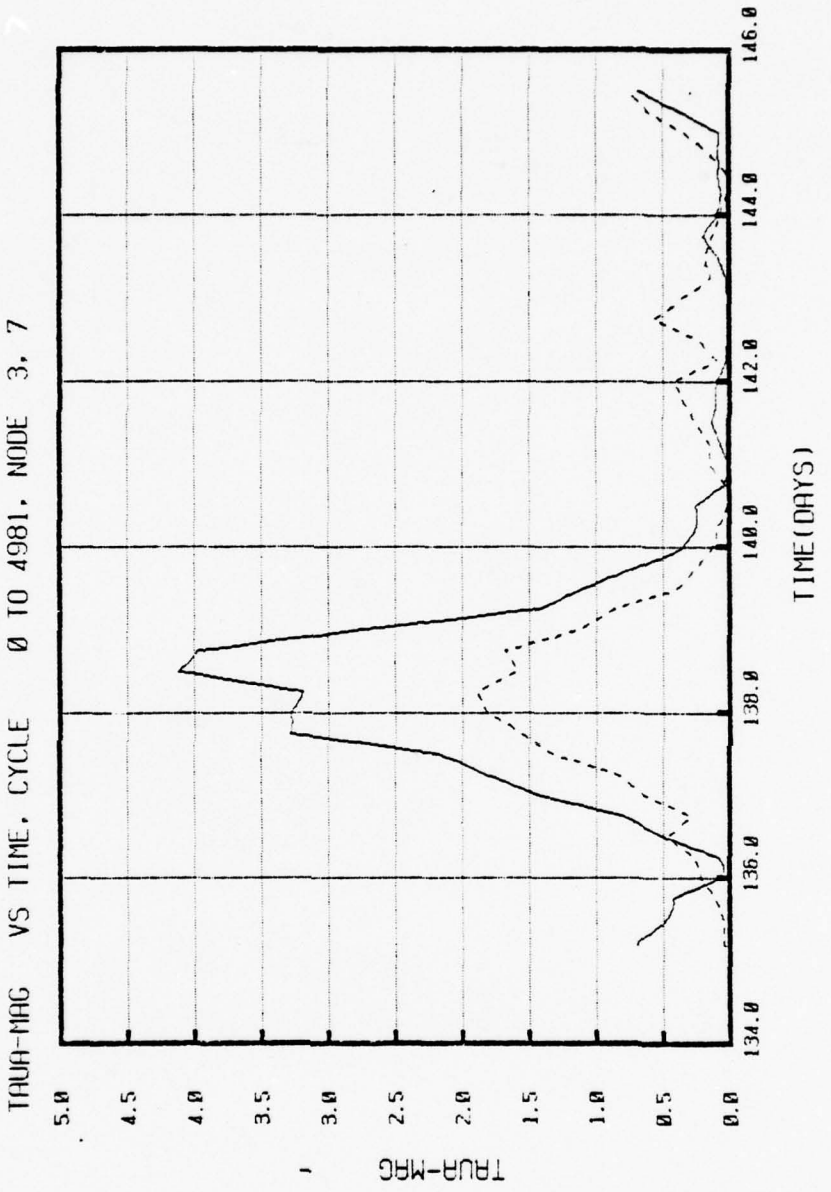


Figure 12a. Computed air stress magnitude (TAUA-MAG) from AIDJEX field (solid line) and FNWC field (dashed line) at node 3,7 for days 15 to 25 May 1975. Units are dynes/cm^2.

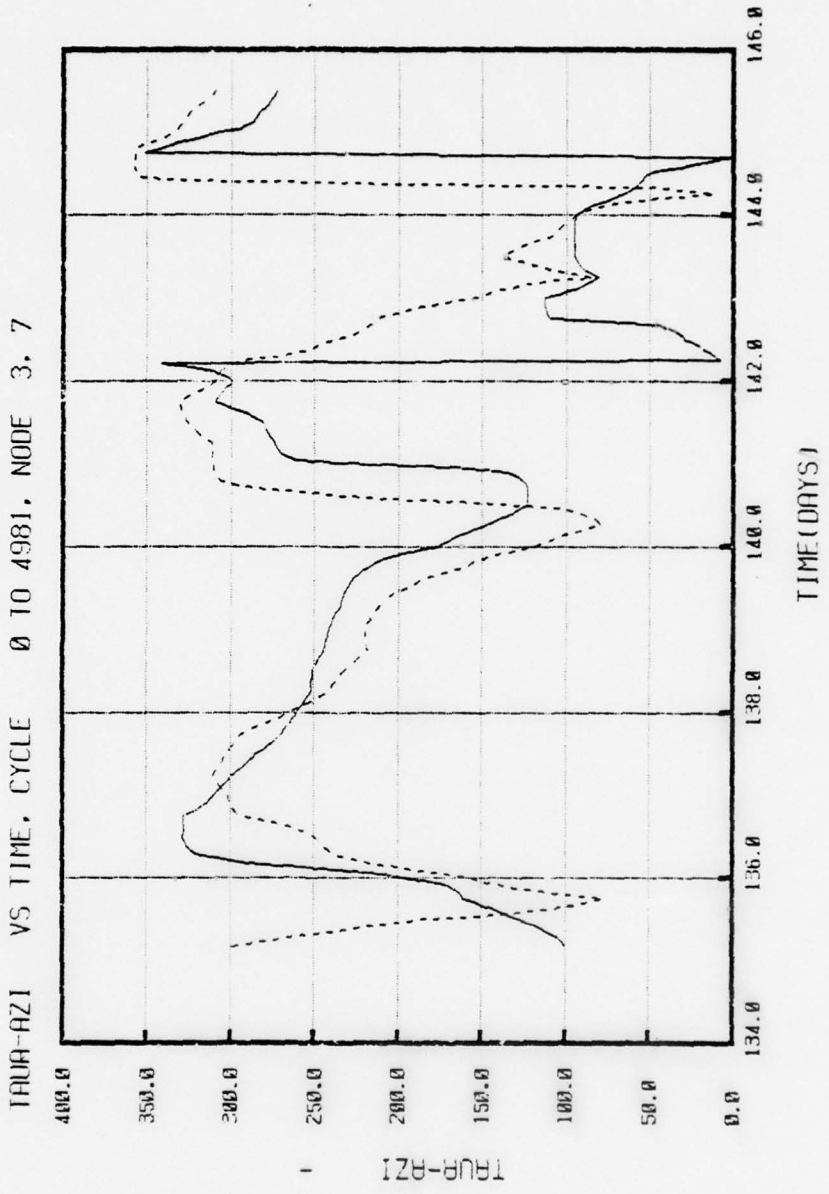


Figure 12b. Computed air stress direction (TAUA-DIR) from AIDJEX field (solid line) and FNWC field (dashed line) at node 3,7 for days 15 to 25 May 1975. Units are degrees true.

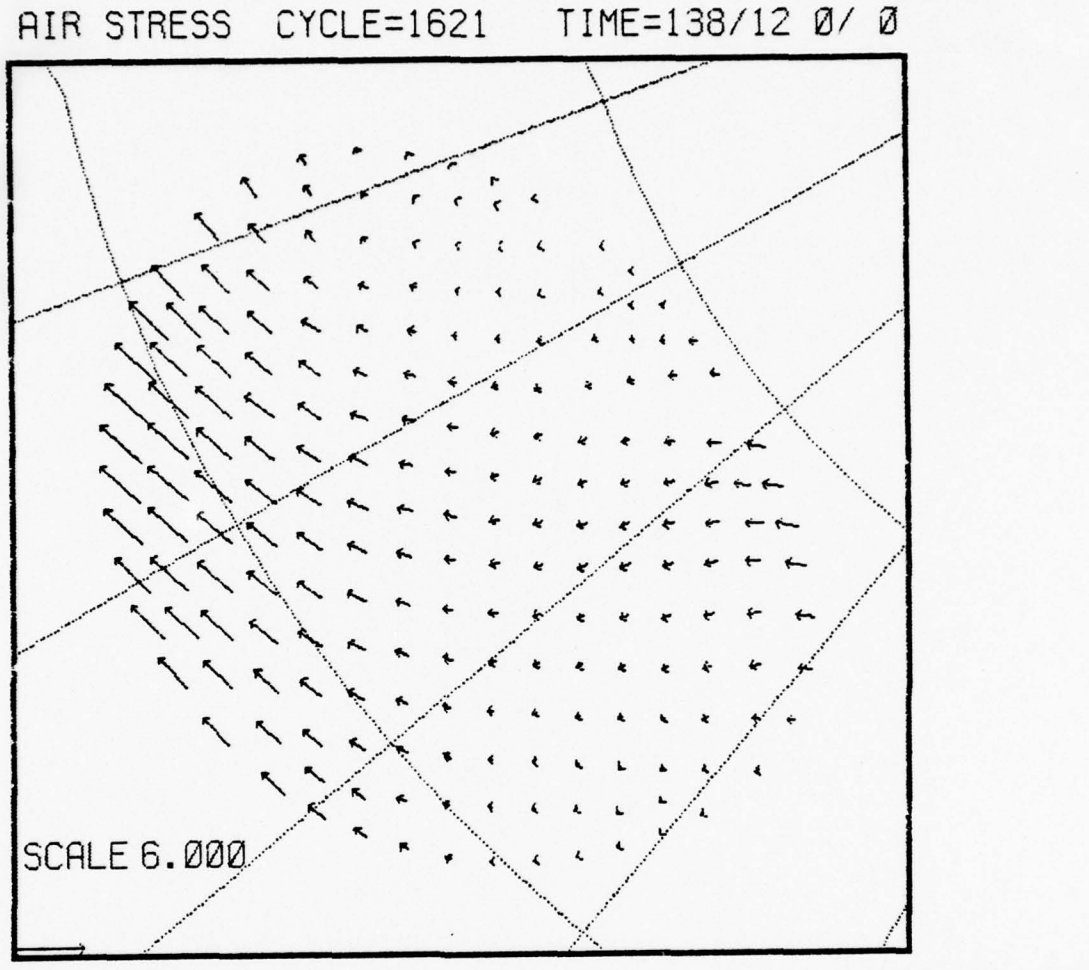


Figure 13. AIDJEX computed air stress field at 1200GMT 18 May 1975. Scale vector represents 6 dynes/cm^2.

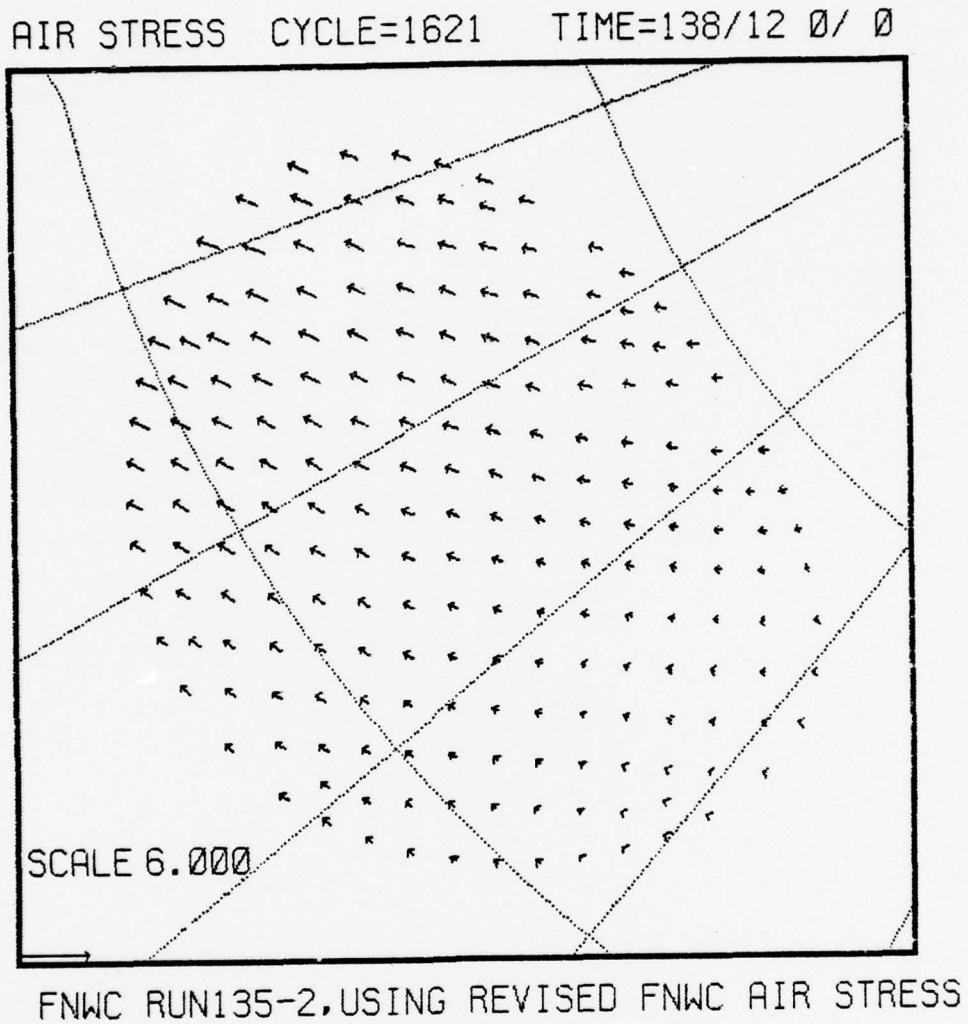


Figure 14. FNWC computed air stress field at 1200GMT 18 May 1975. Scale vector represents 6 dynes/cm^2.

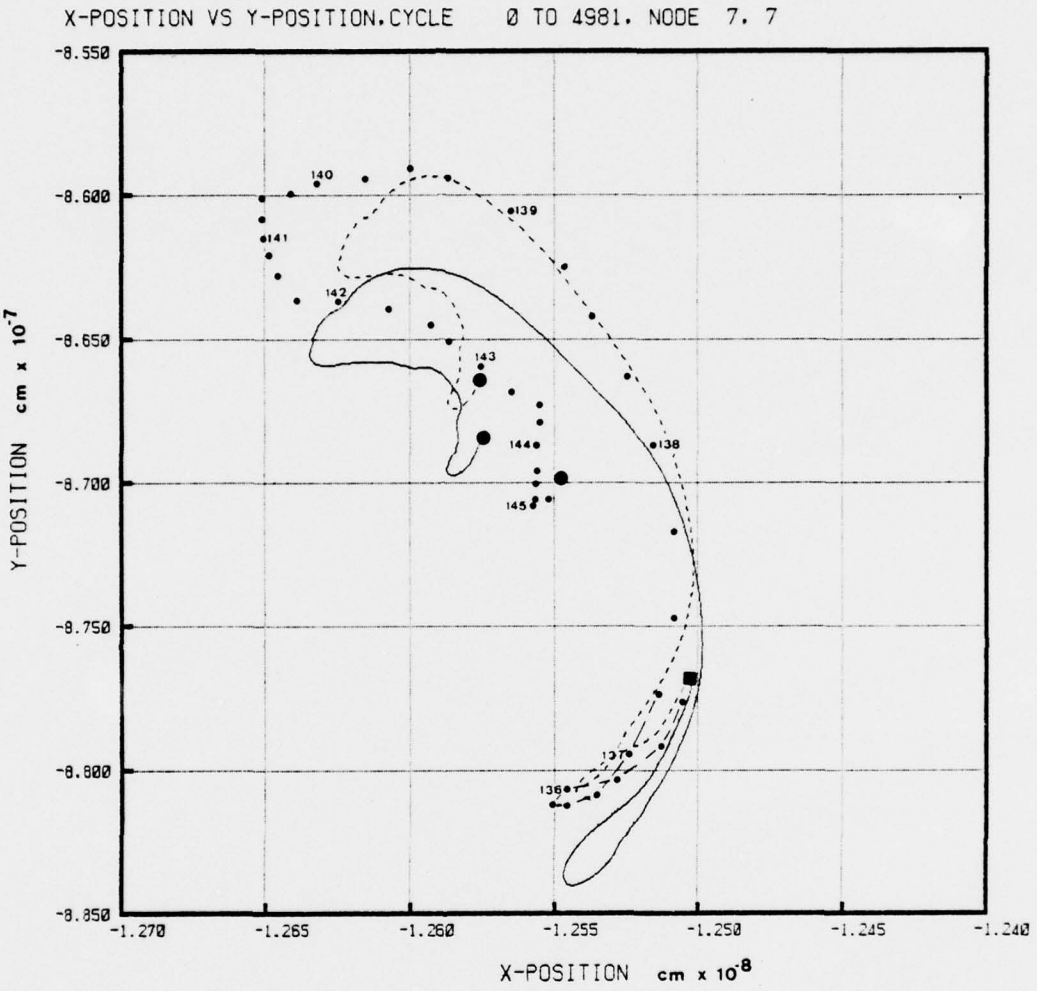


Figure 15. Trajectories of AIDJEX main camp from 15 to 25 May 1975 for AIDJEX simulation (solid line) and FNWC simulation (dashed line). (■) Starting position, (●) ending position, (•) actual measured position every six hours with AIDJEX dates indicated. Grid spacing is 5 km/div.

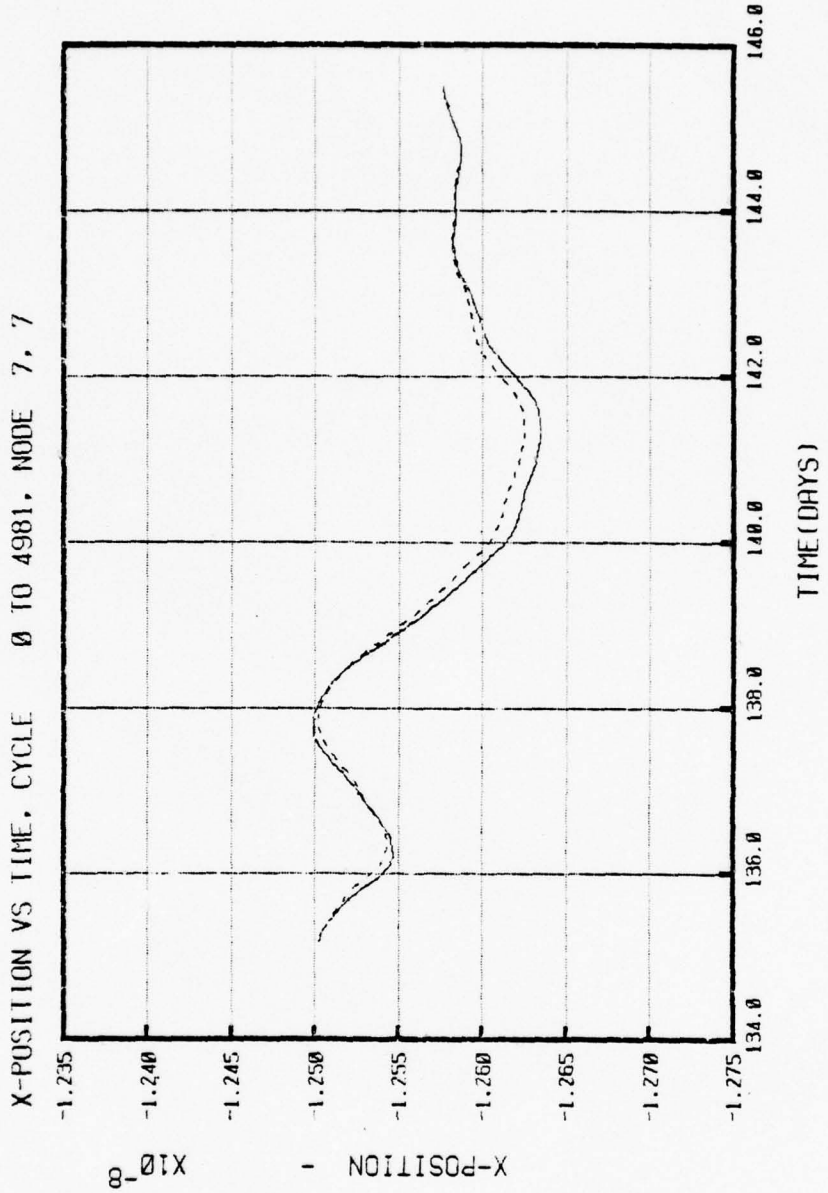


Figure 16a. X - Position time series of AIDJEX main camp as computed by AIDJEX simulation (solid line) and FNWC simulation (dashed line). Ordinate spacing 5 km/div.

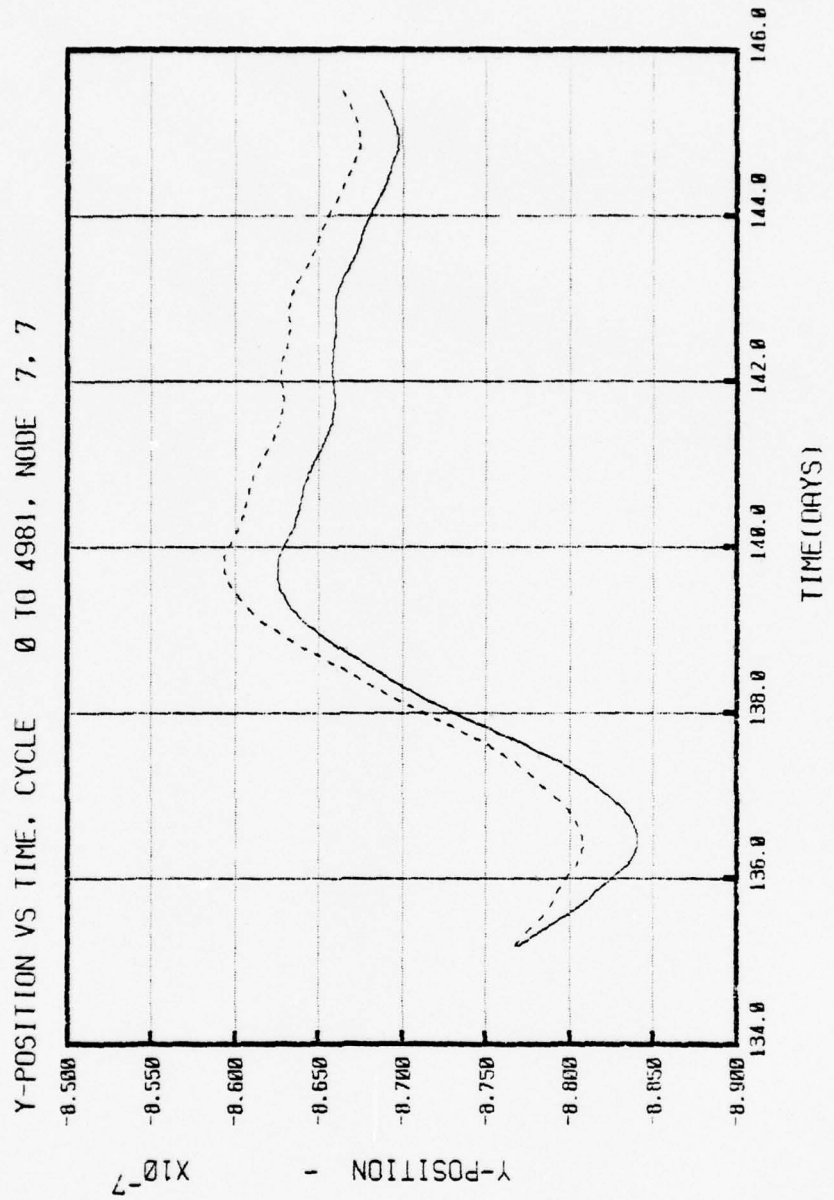


Figure 16b. Y - Position time series of AIDJEX main camp as computed by AIDJEX simulation (solid line) and FNWC simulation (dashed line). Ordinate spacing 5 km/div.

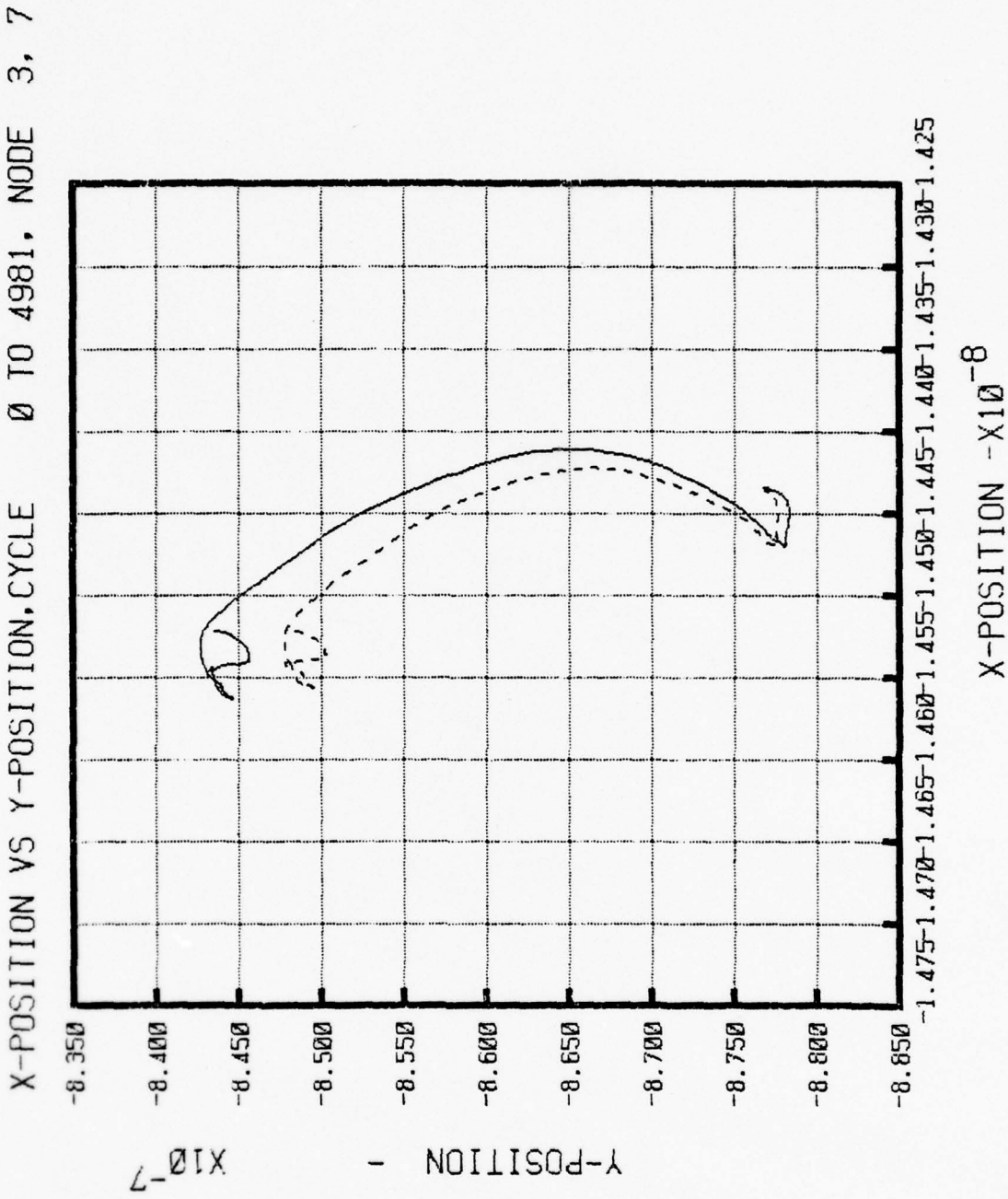


Figure 17. Trajectories of node 3,7 from 15 to 25 May 1975 for AIDJEX simulation (solid line) and FNWC simulation (dashed line). Grid spacing 5 km/div.

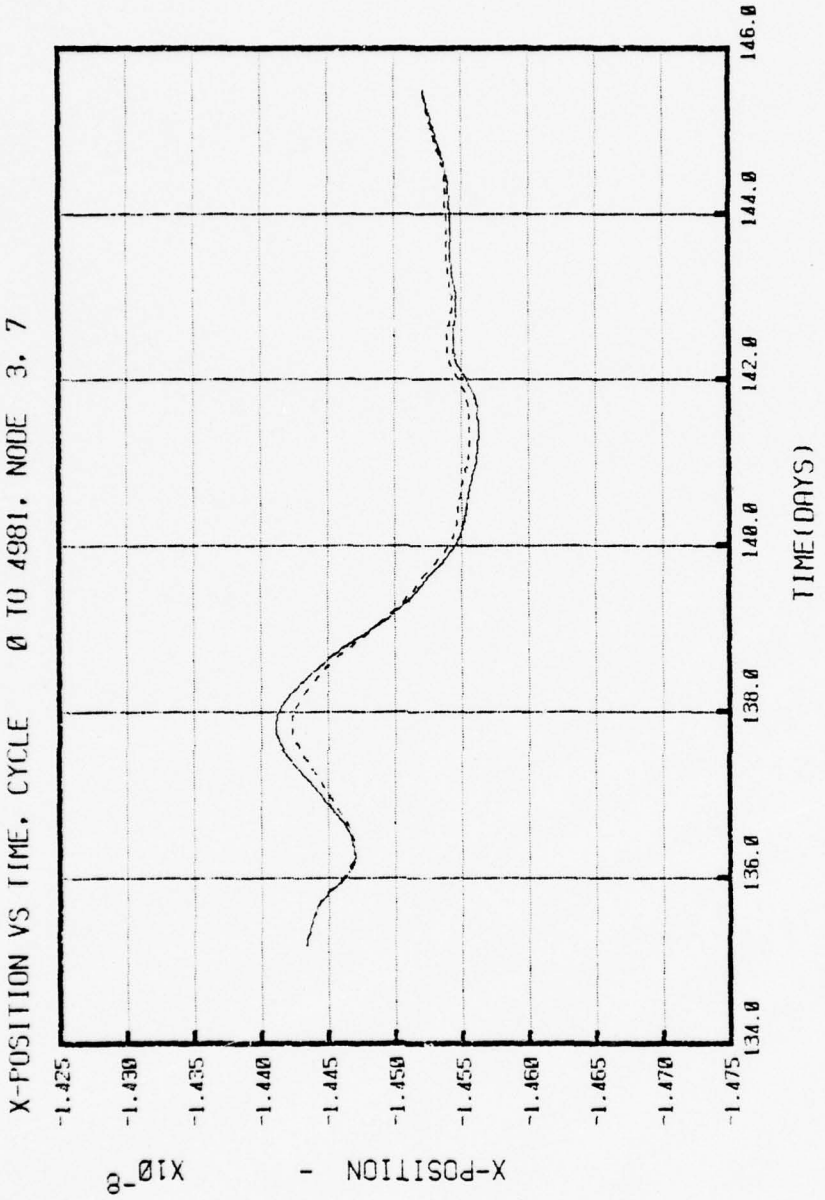


Figure 18a. X - Position time series of node 3,7 as computed by AIDJEX simulation (solid line) and FNWC simulation (dashed line). Ordinate spacing is 5 km/div.

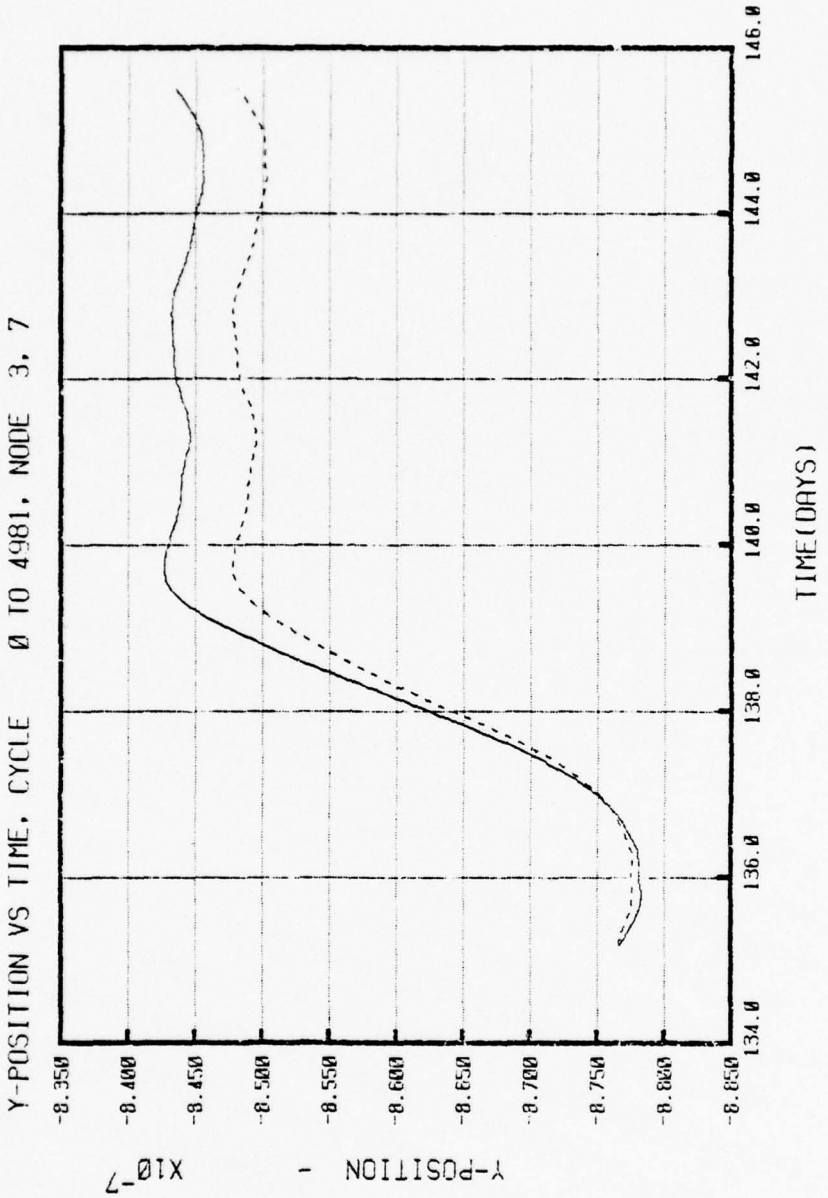


Figure 18b. Y - Position time series of node 3,7 as computed by AIDJEX simulation (solid line) and FNWC simulation (dashed line). Ordinate spacing is 5 km/div.

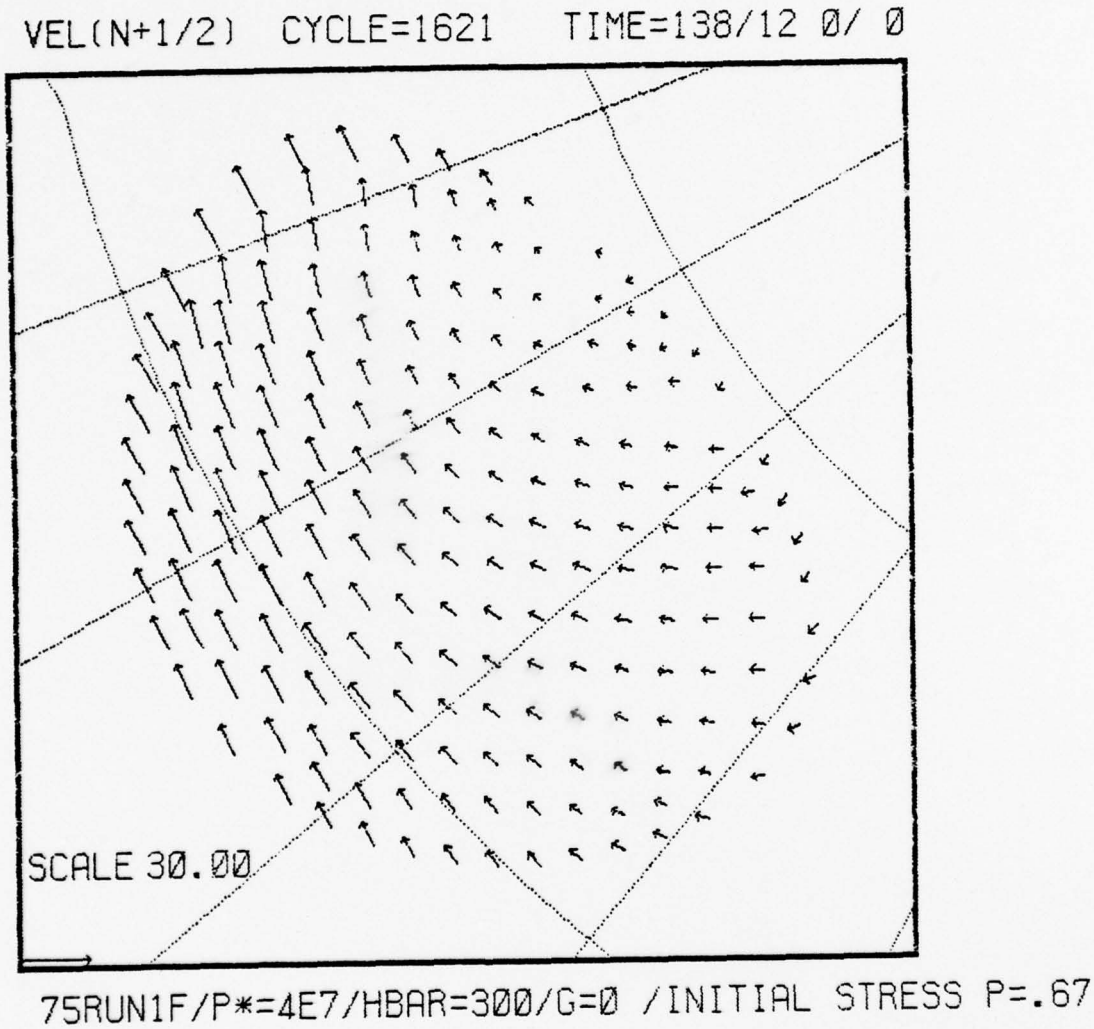


Figure 19. AIDJEX computed velocity field at 1200GMT 18 May 1975. Scale vector represents 30 cm/sec.

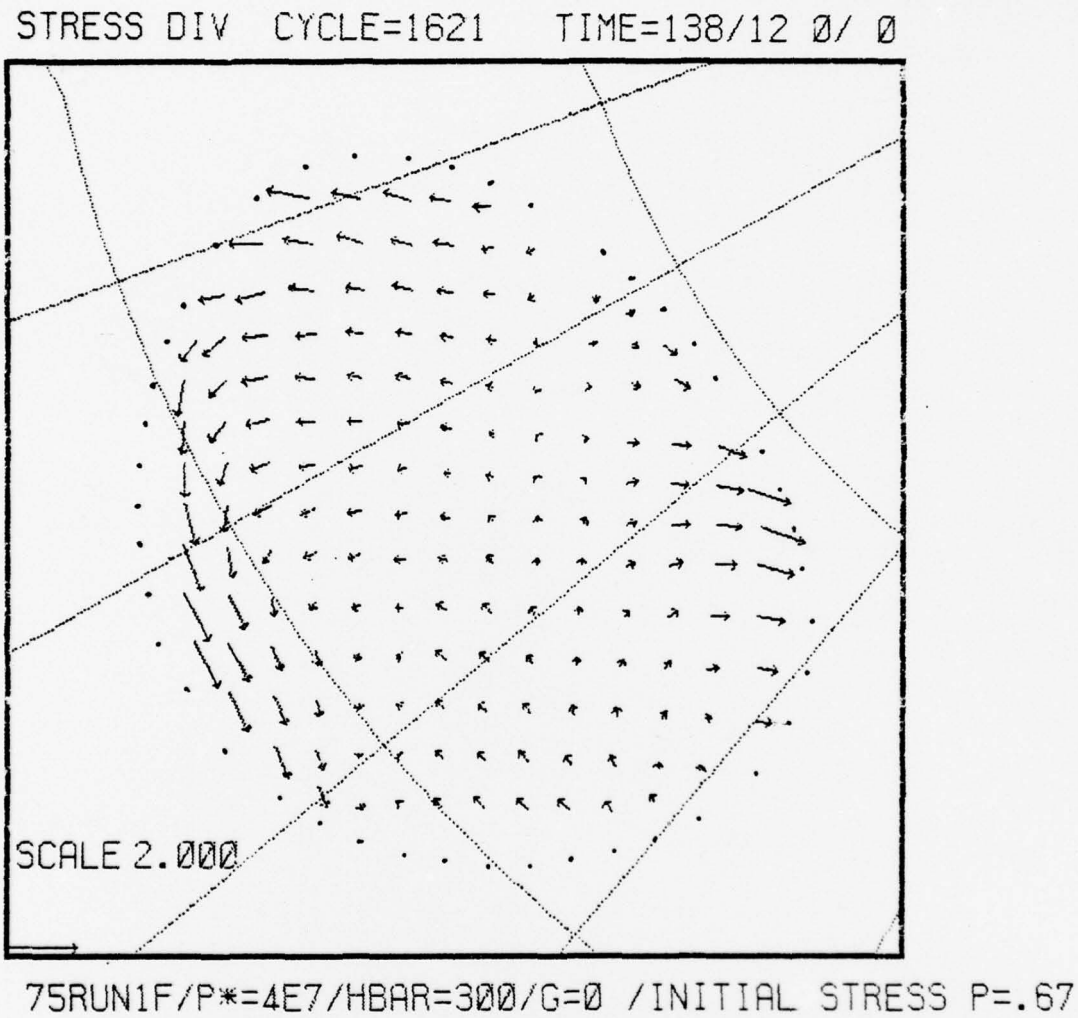


Figure 20. AIDJEX computed stress divergence field at 1200GMT 18 May 1975. Scale vector represents 2 dynes/cm^2.

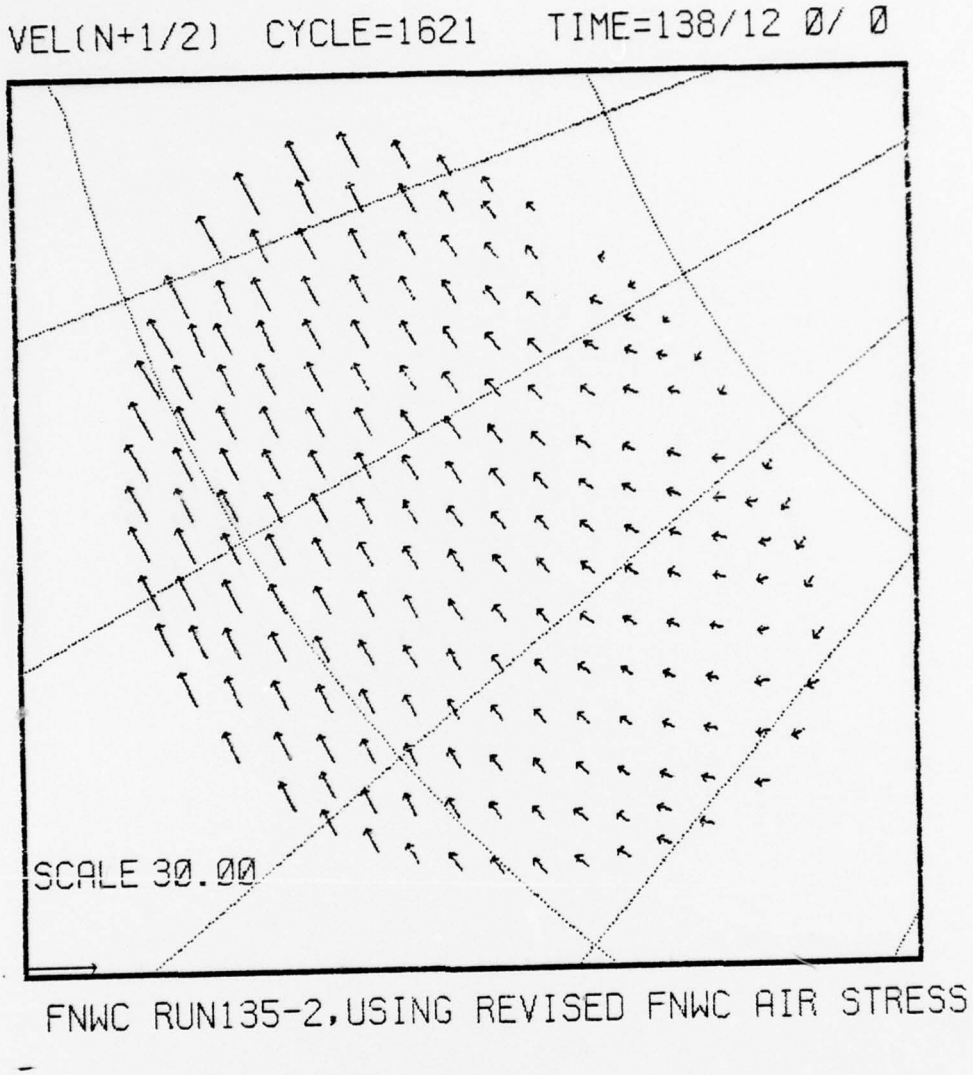


Figure 21. FNWC computed velocity field at 1200GMT 18 May 1975. Scale vector represents 30 cm/sec.

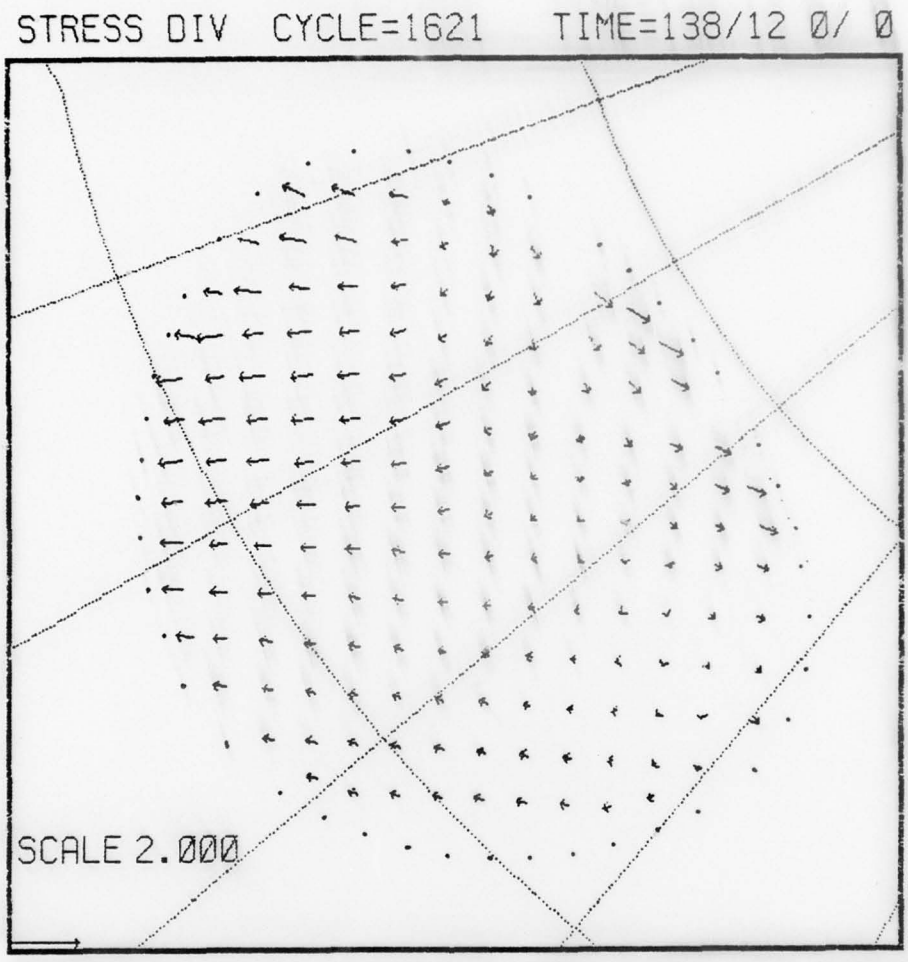


Figure 22. FNWC computed stress divergence field at 1200GMT 18 May 1975. Scale vector represents 2 dynes/cm^2.

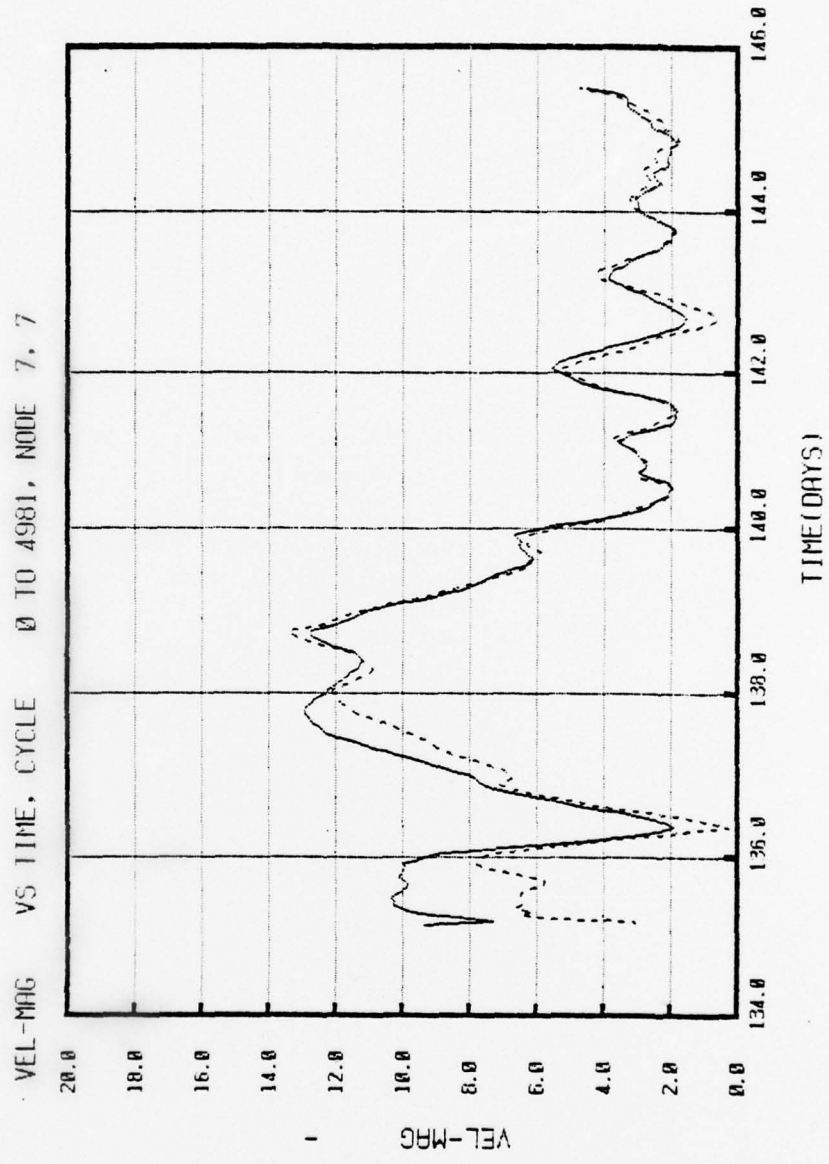


Figure 23a. Velocity magnitude of AIDJEX main camp as computed by AIDJEX simulation (solid line) and FNWC simulation (dashed line). Speed units are cm/sec.

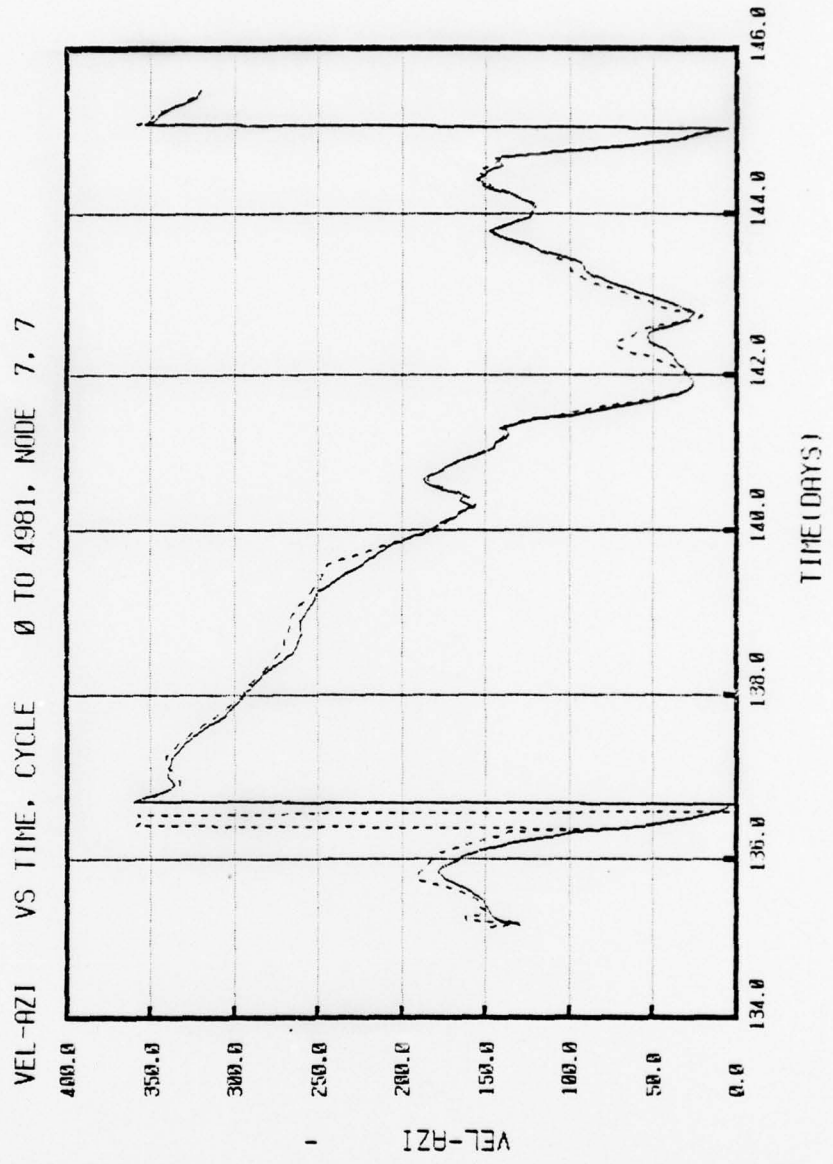


Figure 23b. Velocity direction of AIDJEX main camp as computed by AIDJEX simulation (solid line) and FNWC simulation (dashed line). Direction units are degrees true.

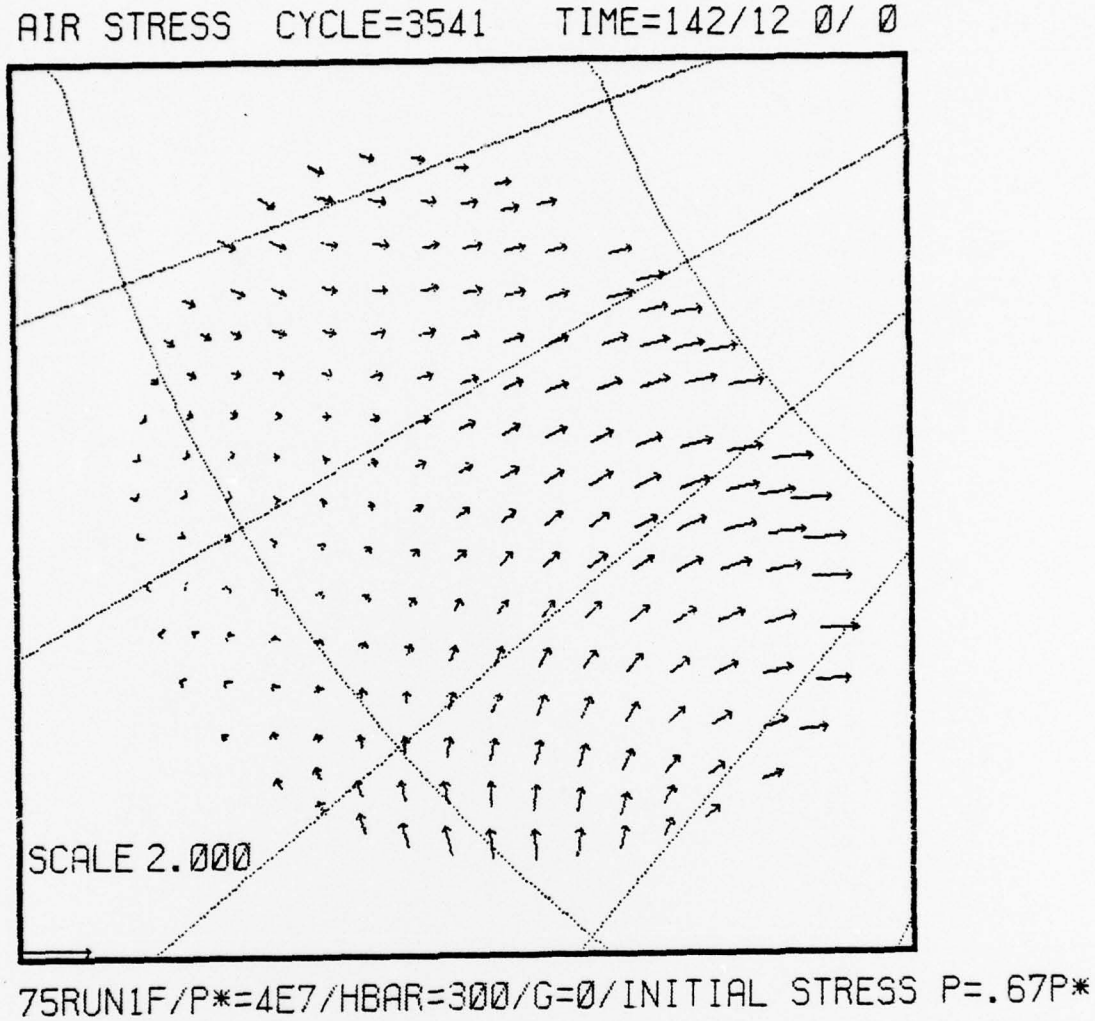


Figure 24. AIDJEX computed air stress field at 1200GMT 22 May 1975. Scale vector represents 2 dynes/cm^2.

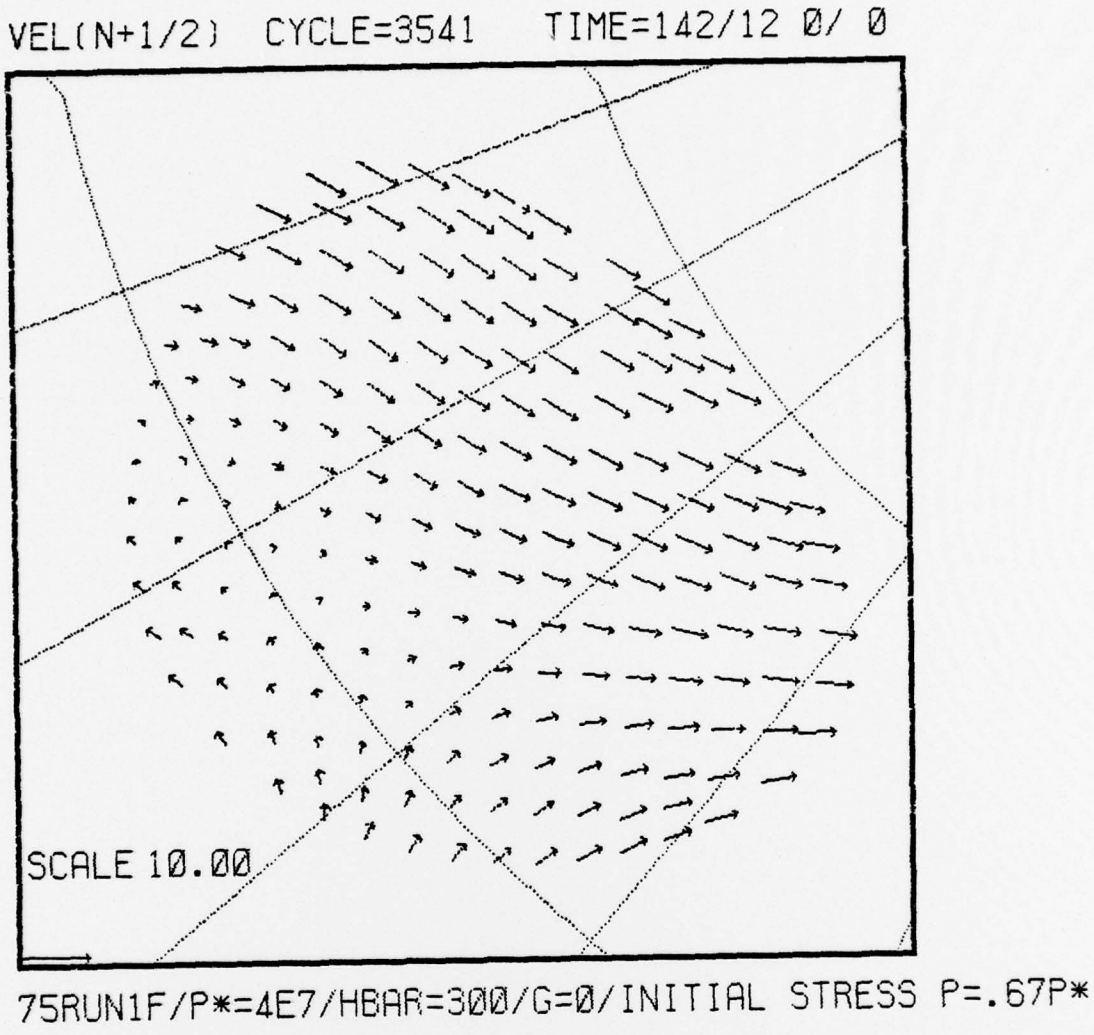


Figure 25. AIDJEX computed velocity field at 1200GMT 22 May 1975. Scale vector represents 10 cm/sec.

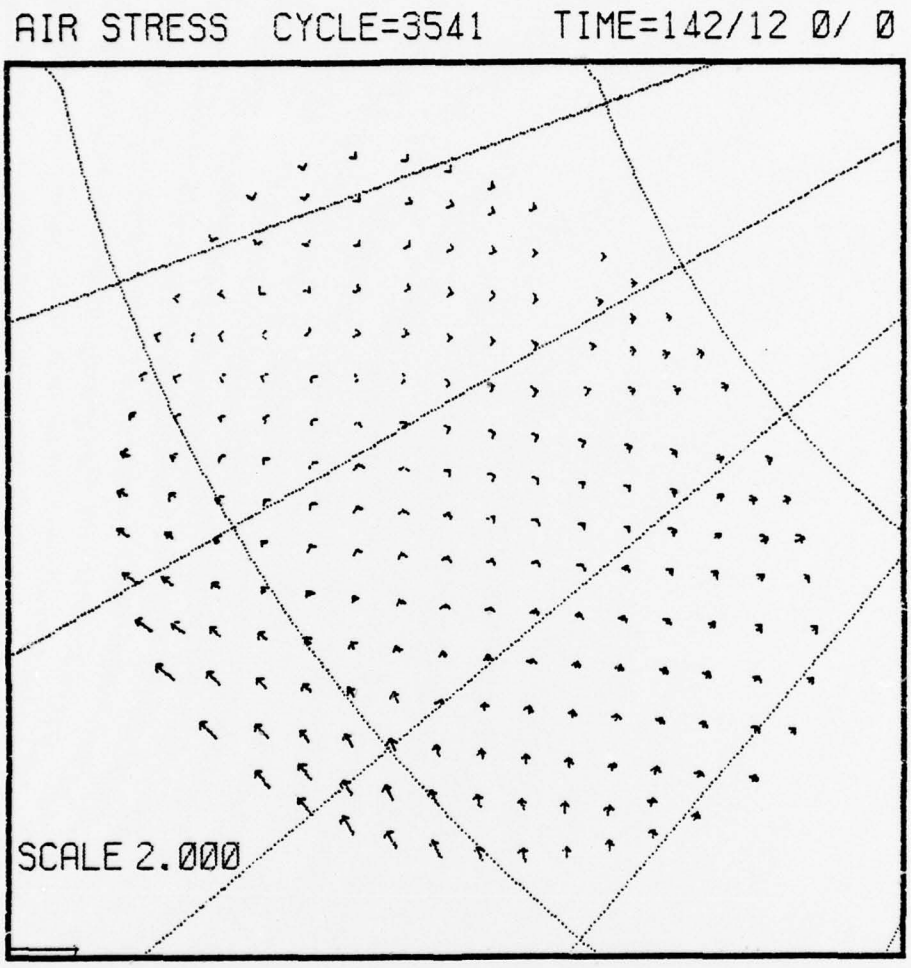


Figure 26. FNWC computed air stress field at 1200GMT 22 May 1975. Scale vector represents 2 dynes/cm^2.

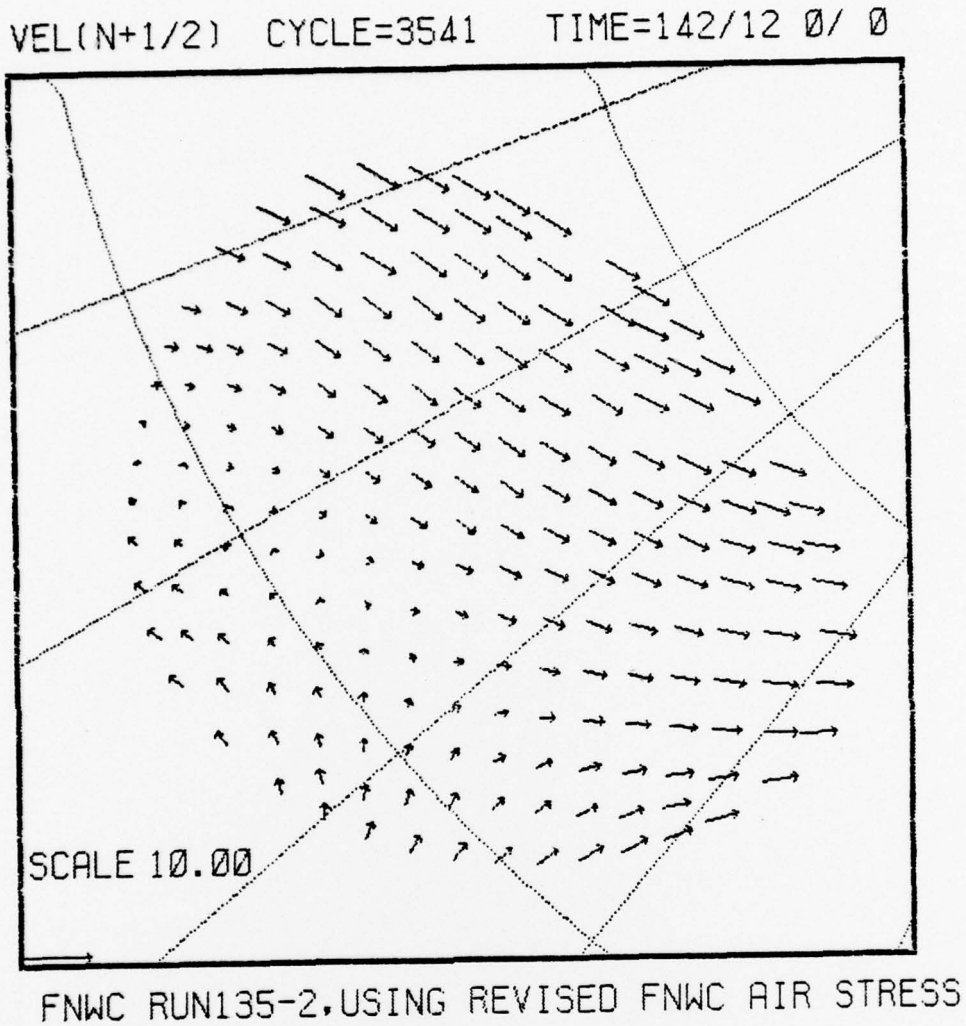


Figure 27. FNWC computed velocity field at 1200GMT 22 May 1975. Scale vector represents 10 cm/sec.

BIBLIOGRAPHY

AIDJEX, "First Data Report," AIDJEX Bulletin, no. 32, June 1976.

Anonymous, Sea Technology, V. 18, no. 5, p. 39-40, May 1977.

Barnett, G., "A Practical Method of Long Range Ice Forecasting for the North Coast of Alaska," Technical Report 1, Fleet Weather Facility, Suitland, Maryland, March 1976.

Campbell, William J., "The Wind-Driven Circulation of Ice and Water in a Polar Ocean," Journal of Geophysical Research, v. 70, no. 14, p. 3279-3301, July 1965.

Colony, Roger, "The Simulation of Arctic Sea Ice Dynamics," AIDJEX Bulletin, no. 31, March 1976.

Coon, M. D., R. Colony, R. S. Pritchard, and D. A. Rothrock, "Calculations to Test a Pack Ice Model," AIDJEX Bulletin, no. 31, March 1976.

Coon, M. D., R. T. Hall, and R. S. Pritchard, "Prediction of Arctic Ice Conditions for Operations," Offshore Technology Conference, Preprints, 1977.

Diachok, O. I., "Recent Advances in Arctic Hydroacoustics," Naval Research Reviews, May 1976.

Fukutomi, T., "On the Steady Drift Current and Steady Drift of Sea Ice due to Wind on the Frozen Sea," Study of Sea Ice, Report No. 14, Low Temperature Science Research Laboratory, Hokkaido University, Hokkaido, Japan, October 1948.

Gerson, D. J., "A Numerical Ice Forecasting System," Reference Publication, no. 8, U. S. Naval Oceanographic Office, v. 138, December 1975.

Gerson, D. J., and L. S. Simpson, "Wind Drift of Sea Ice," Reference Publication, no. 8S, U. S. Naval Oceanographic Office, September 1976.

Hibler, W. D., III, "Modeling Pack Ice as a Viscous-Plastic Continuum: Some Preliminary Results," ICSI/AIDJEX Symposium on Sea Ice Process and Models, Seattle, Wa., September 1977.

Holl, M. M., and B. R. Mendenhall, "Field by Information Blending, Sea-level Pressure Version," FNWC Technical Note, no. 72-2, March 1972.

Knodle, William C., A Computer Program for Forecasting the Wind Drift of Sea Ice, Master's Thesis, Naval Postgraduate School, Monterey, CA, 1964.

Maykut, Gary A., "Energy Exchange Over Young Sea Ice in the Central Arctic," AIDJEX Bulletin, no. 36, March 1976.

Monterey Peninsula Herald, "USSR Plans to Create Arctic Circle Shipping Route," p.7, Monterey, CA, Aug. 19, 1977.

Nansen, F., "The Oceanography of the North Polar Basin," The Norwegian Polar Expedition, 1893-1896: Scientific Results, v. 3, p. 357-386, 1902.

Orvig, S., ed., "World Survey of Climatology," Climate of the Polar Regions, v. 14, Elsevier Publishing Company, 1970.

Pritchard, R. S., M. D. Coon, M. G. McPhee and E. Levitt, "Winter Ice Dynamics in the Nearshore Beaufort Sea," Appendix 3 in Annual Report on contract 03-50-022-67, no. 5 to Outer Continental Shelf Environmental Assessment Program, University of Alaska, Fairbanks, Alaska, April 1, 1977.

Pritchard, R. S., and R. Colony, "A Difference Scheme for the AIDJEX Sea Ice Model," AIDJEX Bulletin, no. 31, March 1976.

Sater, John E., A. G. Ronhovde, and L. C. Van Allen, Arctic Environment and Resources, The Arctic Institute of North America, 1971.

Shuleikin, V. V., Fizika moria, izdamie tret'e. (Physics of the Sea, 3rd Ed.), Press of the Academy of Sciences of the USSR, Moscow, USSR, 1953.

Skiles, F. L., "Empirical Wind Drift of Sea Ice," Arctic Drifting Stations, J. E. Sater, Ed., The Arctic Institute of North America, 1968.

Sverdrup, H. U., "The Wind Drift of the Ice on the North Siberian Shelf," The Norwegian North Polar Expedition with the Maud, 1918-1925: Scientific Results, v. 4, p. 46, 1929.

Synhorst, G. E., "Soviet Strategic Interest in the Maritime Arctic," U. S. Naval Institute Proceedings, Naval Review Edition, 1973.

Thorndike, A. S., and J. Y. Cheung, "AIDJEX Measurements of Sea Ice Motion, 11 April 1975 to 14 May 1976," AIDJEX Bulletin, no. 35, January 1977.

Urick, Robert J., Principles of Underwater Sound, McGraw-Hill, 1975.

U. S. Naval Weather Service, Numerical Environmental Products Manual, NAVAIR 50-10-522, 1 June 1975.

Walsh, J. E., "Ice Forecasting Limitations Imposed by the Accuracy of Atmospheric Prediction Models," AIDJEX Bulletin, no. 36, May 1977.

Zubov, N. N., L'dy Arktiki (Arctic Ice), Northern Sea Route Directorate Press, Moscow, USSR, 1945.

INITIAL DISTRIBUTION LIST

		No. Copies
1.	Defense Documentation Center Cameron Station Alexandria, VA 22314	2
2.	Library (Code 0142) Naval Postgraduate School Monterey, CA 93940	2
3.	Department of Oceanography, Code 68 Naval Postgraduate School Monterey, CA 93940	3
4.	Professor Warren W. Denner, Code 68Dw Department of Oceanography Naval Postgraduate School Monterey, CA 93940	3
5.	LT Larry D. Ashim 649 Hillcrest Ave. Pacific Grove, CA 93950	2
6.	Professor Robert J. Renard, Code 63Rd Department of Meteorology Naval Postgraduate School Monterey, CA 93940	1
7.	Oceanographer of the Navy Hoffman Building No. 2 200 Stovall Street Alexandria, VA 22332	1
8.	Office of Naval Research Code 410 NORDA NSTL Station, MS 39529	1
9.	Dr. Robert E. Stevenson Scientific Liaison Office, ONR Scripps Institution of Oceanography La Jolla, CA 92037	1
10.	Library, Code 3330 Naval Oceanographic Office Washington, D.C. 20373	1
11.	SIO Library University of California, San Diego P.O. Box 2367 La Julla, CA 92037	1

12. Department of Oceanography Library — 1
University of Washington
Seattle, WA 98105

13. Department of Oceanography Library — 1
Oregon State University
Corvallis, OR 97331

14. Commanding Officer — 1
Fleet Numerical Weather Central
Monterey, CA 93940

15. Commanding Officer — 1
Naval Environmental Prediction
Research Facility
Monterey, CA 93940

16. Department of the Navy — 1
Commander Oceanographic System Pacific
Box 1390
FPO San Francisco 96610

17. Director — 1
Naval Oceanography and Meteorology
National Space Technology Laboratories
NSTL Station, MS 39529

18. Naval Oceanographic Research and — 1
Development Activity
National Space Technology Laboratories
NSTL Station, MS 39529

19. AIDJEX — 1
4059 Roosevelt Way N.E.
Seattle, WA 98105

20. Commanding Officer — 1
Fleet Weather Facility
Suitland, MD 20023

21. U. S. Army Cold Regions Research — 1
Laboratory
Hanover, NH 03755

22. Office of Naval Research (Code 461) — 2
Department of the Navy
Arlington, VA 22217

23. Diane B. Chace, Code 68 — 1
Department of Oceanography
Naval Postgraduate School
Monterey, CA 93940